SYNTHESIS AND CHARACTERIZATION OF METAL COMPLEXES OF 2-BENZOYLPYRIDINE AND DI-2-PYRIDYL KETONE SCHIFF BASE LIGANDS DERIVED FROM *S*-METHYLDITHIOCARBAZATE FRAGMENT AND ITS APPLICATION TO BIOLOGICAL ACTIVITY TOWARD *P. FALCIPARUM*

A THESIS SUBMITTED IN PARTIAL FULFILMENT

OF THE REQUIREMENTS FOR THE DEGREE OF

MASTER OF SCIENCE

OF

THE UNIVERSITY OF NAMIBIA

BY

ALINA UUSIKU

(200518321)

November 2015

Supervisor: Professor E. M. R. Kiremire

Co-supervisor: Dr Likius S. Daniel

ABSTRACT

The synthesis, characterization, spectroscopic and biological evaluation of 2-benzoylpyridine-*s*-methyldithiocarbazate (HL^1) and di-2-pyradylketone-*s*-methyldithiocarbazate (HL^2) with selected metal ions of copper (II), zinc (II), cadmium (II), nickel (II), iron (II) and cobalt (II). The ligands, HL^1 and HL^2 were synthesized by an acid catalyzed condensation reaction of *s*-methyldithiocarbazate with 2-benzoylpyradine and di-2-pyradylketone respectively. The reaction of metal salts with the resultant ligands, HL^1 and HL^2 produced solid complexes. The ligands and the complexes were characterized by means of Elemental Analysis (EA), Fourier Transform Infrared (FT-IR) spectroscopy, Nuclear Magnetic Resonance (^{1}HNMR) spectroscopy. HL^1 and HL^2 ligands coordinated in their deprotonated form through one of the pyridine nitrogen atoms, the azomethine nitrogen atom and the thiolate sulfur atom, thus HL^1 and HL^2 behaved as tridentate *N, N, S* chelate with all coordinated respective metal ions centers. The synthesized ligands and their corresponding metal complexes were screened for anti-*plasmodial* activities against malaria parasite using *in vitro* technique. Using IC_{50} (half inhibitory concentration) to measure the biological strength of the compounds. It revealed that ligands were more biological active toward NF54 strain of *P. falciparum* than their corresponding metal complexes and that HL^1 have increased antiplamodial activity than its counterpart HL^2.

Table of Contents

List of Tables

List of Schemes

List of Figures

List of abbreviations and symbols used

TSC	Thiosemicarbazones
2-PT	Pyridine-2-thiosemicarbazone
RR	Ribonucleotide Reductase
HL^1	2-benzoylpyridine-s-methyldithicarbazate
HL^2	di-2-pyridylketone-s-methydithiocarbazate
H_2O	water
MeOH	methanol
EtOH	ethanol
Et_2O	diethylether or ethoxyethane
$CHCl_3$	chloroform
DMF	dimethylformamide
DMSO	Dimethyl Sulfoxide
M.P	Melting Point
EA	Elemental analysis
HNMR	Proton Nuclear Magnetic Resonance
EI-MS	Electron Ionization Mass Spectroscopy
Anal. Cal	Analytical Calculations
Py	Pyridyl

TMS	Tetramethylsilane
CQ	Chloroquine
CQS	Chloroquine sensitive
Ppm	Parts per million
ºC	degree celcius
δ	chemical shift
≤	less than or equal to
±	plus or minus

Acknowledgements

I owe my deepest gratitude and it gives me great pleasure in acknowledging the support and help of the following people for making this study possible.

I would like to express my sincere gratitude to my supervisor Prof E. M. R. Kiremire for the continuous support during my M.Sc. course work and research study, for his patience, motivation, enthusiasm and immense knowledge. His guidance helped me in all the time of research and writing of this thesis. I could not have imagined having a better advisor and mentor for my M.Sc. study.

My sincere thanks go to my co-supervisor Dr Daniel Likius for his inspiration, encouragement and insightful comments. He has made available his support in a number of ways throughout this study.

It's a pleasure to thank Dr. Nchinda of the University of Cape Town for putting aside his own research busy schedule, in order to assist with spectroscopic analysis and biological studies for this research.

I consider it an honor to work with my friend Mr. Phillip Hishimone. I am very thankful for all the laboratory assistances he offered me. I am also very grateful to all my friends and family for their love and understanding throughout this study.

I am indebted to all staff members of the department of Chemistry and Biochemistry at the University of Namibia for their valuable invested time and support during this study.

To my late unbiological mother, Alma Nangula Johannes "Mukuto gwaNaambo"

(1945-2013)

Conference presentations

- ✓ A. Uusiku. Synthesis and characterization of metal complexes of 2-benzoylpyridine and di-2-pyridyl ketone schifff base ligands derived from s-methyldithiocarbazate. 2nd Annual Science Research Conference. 30-31 October 2014, Windhoek, Namibia.

- ✓ A. Uusiku, E. M. R. Kiremire and L. Daniels. Synthesis and characterization of metal complexes of di-2-pyridyl ketone Schiff base ligands derived from s-methyldithiocarbazate fragment. SPACC. August 2015, Windhoek and Ongwediva, Namibia.

- ✓ A. Uusiku*, E. M. R. Kiremire and L. Daniels. The study of metal complexes of di-2-pyridyl ketone Schiff base ligands derived from s-methyldithiocarbazate fragment and its application to biological activity toward *P. Falciparum*. 3rd Annual Science Research Conference. November 2015, Windhoek, Namibia.

Declarations

I, UUSIKU ALINA declare hereby that this study is a true reflection of my own research, and that this work, or part thereof has not been submitted for a degree in any other institution of higher education.

No part of this thesis/dissertation may be reproduced, stored in any retrieval system, or transmitted in any form, or by means (e.g. electronic, mechanical, photocopying, recording or otherwise) without the prior permission of the author, or The University of Namibia in that behalf.

I, UUSIKU ALINA grant The University of Namibia the right to reproduce this thesis in whole or in part, in any manner or format, which The University of Namibia may deem fit, for any person or institution requiring it for study and research; providing that The University of Namibia shall waive this right if the whole thesis has been or is being published in a manner satisfactory to the University.

……. Date……..

Uusiku Alina

CHAPTER 1: INTRODUCTION

1.1 General introduction

According to the World Health Organization (WHO), there are 300–500 million clinical cases of malaria each year, resulting in an alarming rate of about 1.5–2.0 million deaths annually, however, it is estimated that this death rate is likely to increase further because of the high level of drug resistance to most of the clinically used antimalarials drugs (Bahl *et al*., 2010).

Malaria is a serious mosquito-borne infectious disease in hot countries that comes from the bite of a small female flying insect called mosquito (Steel, 2001). Even though there are precautional measures (e.g mosquito elimination, prevention of bites by sleeping in mosquito nets and medications), there are so many people dying in the world as a result of contracting malaria. The disease is tremendously killing people worldwide and many people are at risk every year and according to Bloland (2001), more than 90% of the 1.5 to 2.0 million deaths attributed to malaria each year occur in African children.

According to de Lima et al. (1999), thiosemicarbazones (figure 1) and their metal complexes are a broad class of biologically active compounds; also it was found that their derivatives are of considerable interest due to their biological activities (Lakovidou, 200l). The use of thiosemicarbazonesp (TSCs) as potential chemotherapeutics is an active area of research (Chellan *et al*., 2010). In this research the thiosemicarbazone based ligands (HL^1 and HL^2) with their corresponding metal complexes were synthesized and tested for possible biological activities.

These compounds have been extensively studied due to wide range of biological activities (Li, 2009). As a result, a large number of organic and metal-organic compounds derived from these thiosimcarbazone have been the subject of most structure and medicinal studies (Kizilcikli et al., 2007).

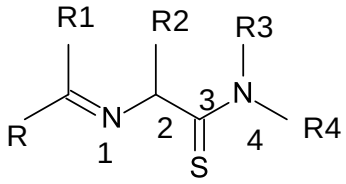

Figure 1: General structures of thiosemicarbazone ligands. Where R=0, 1, 2, 3 or 4 can be alkyl, aryl or H.

1.2 The importance of ligands and metal complexes

Known ligands such as 2-acetylpyridine thiosemicarbazones possess anti-trypanosomal, antibacterial, antiviral and anti-leukemic properties (Scovill, 1983). The attention has centered upon the antimalarial effects of these compounds, their analogues and derivatives, a program of modification has been undertaken in order to develop agents with greater efficacy against drug-resistant malaria (Scovill, 1983).

Cancer remain among the most widespread diseases and difficult to treat often causing poor general conditions of patients and are characterized by a high death rate (Ott, 2008). However the same applies to malaria parasitic disease. Among others, gold metal complexes have been used in recent years and the interest in non-platinum metal complexes for cancer chemotherapy has been rapidly growing (Ott, 2008).

Contrastingly this has been stimulated by the possibility to develop new agents with a mode of action and clinical profile different from the established platinum metallodrugs (Ott, 2008):

Thiosemicarbazones display a broad spectrum of biological activities; hence so much effort has been devoted to their structural variations for achieving the ultimate goal of medicinal applications (Pingaew, 2010). The antitumor activity of such thiosemicarbazone compounds was revealed in their ability to inhibit ribonucleotide reductase (RR), a necessary enzyme for DNA synthesis (Pingaew, 2010). However, isoquinoline-1-carboxaldehyde thiosemicarbazone a 3, 4-benzo derivative of pyridine-2-carboxaldehyde thiosemicarbazone (2-PT), was shown to be a significantly more potent inhibitor of RR than the parent compound and less toxic (Pingaew, 2010). The result suggested that the occurrence of a hydrophobic interaction between the benzenoid moiety of isoquinoline-1-carboxaldehyde thiosemicarbazone and the enzyme renders the compound more biological activity (Pingaew, 2010).

CHAPTER 2: LITERATURE REVIEW

2.1 The potential reactivity of Schiff's base with thiosemicarbazones

Schiff's bases are an important class of organic compounds which were first reported by Hugo Schiff in 1864 and by definition this azomethine group (-CH=N-) containing compounds are condensation products of primary amines with carbonyl compounds (Hussain *et al*., 2014). The common structural feature of these compounds is the azomethine group with the general formula RHC = N-R_1, where R and R_1 are alkyl, aryl, cycloalkyl, or heterocyclic groups (Hussain *et al*., 2014).

Schiff bases are generally bi- or tri- dentate ligands capable of forming very stable complexes with transition metals. However these bases of aliphatic aldehydes are relatively unstable and are readily polymerizable while those of aromatic aldehydes, having an effective conjugation system, are more stable (Arulmuruga *et al*., 2010), which is due to the fact that aromatic aldehyde forms more membered ring compounds or complexes than aliphatic aldehyde. In this study aromatic ketones are used as Schiff's bases and their general formation is shown by scheme 1. the stability of metal complexes of Schiff's base ligands can be attributed to hydrazones which according to Eissa (2013), are special group of compounds in the Schiff bases family. These compounds are characterized by the presence of (C=N-N=C) (Eissa, 2013). However it's the additional donor site (C=O) of hydrazone Schiff bases of acyl, and heteroacroyl compounds that make them more flexible and versatile, thus making them good polydentate chelating agents that can form a variety of complexes with

various transition metals (Eissa, 2013). This has attracted the attention of many researchers (Eissa, 2013).

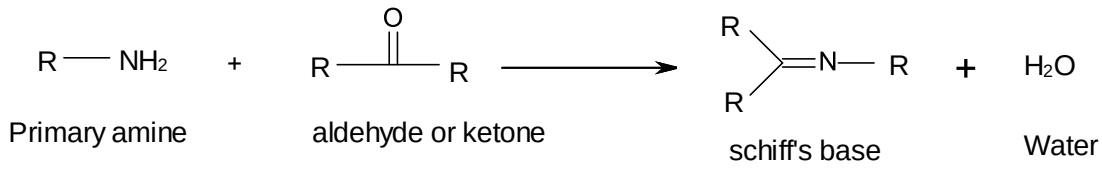

Scheme 1: General reaction scheme of Schiff base formation

2.2 The semicarbazides, thiosemicarbazides, semicarbazones and thiosemicarbazones

2.2.1 The semicarbazides/thiosemicarbazides

Semicarbazides are derivative of urea (figure 2), which plays an important role in the metabolism of nitrogen-containing compounds in animals and they are important pharmacophores in the search for new drugs (Sayin *et al*., 2010), which is for the same reason are studied under this research. Coordination chemistry of semicarbazides/thiosemicarbazides has been a subject of enthusiastic research since they are wide spectrum ligands that can give rise to a great variety of coordination modes (Yousef *et al*., 2015). These compounds also show a wide range of biological properties ranging from anticancer, antitumor, antifungal, antibacterial, antimalarial, antifilarial, antiviral and anti-HIV activities (Yousef *et al*., 2015). Moreover, the biological activities of their complexes could be due to metal ion coordination (Yousef *et al*., 2015). Structurally semicarbazones (figure 3A) differ from

thiosemicarbazones (figure 3B) only by replacing the oxygen atom with a sulphur atom and they are ketone form of semicarbazide (figure 2A) (Pavan *et al*., 2010).

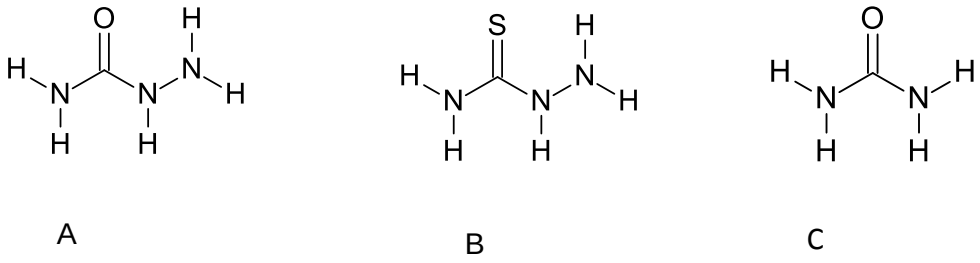

Figure 2: General structures of (A) semicarbazide, (B) thiosemicarbazide and (C) urea

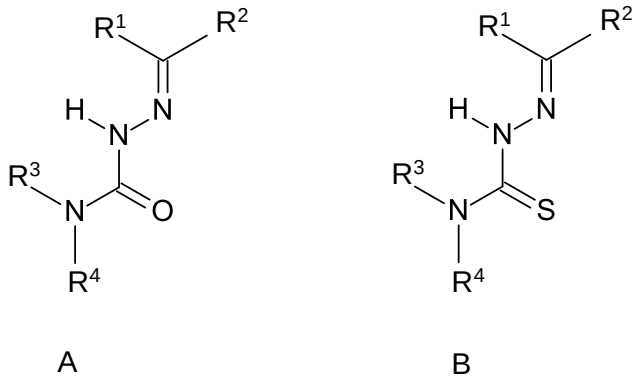

Figure 3: Structure of (A) semicarbazone and (B) thiosemicarbazone, where R^1, R^2, R^3, R^4 = H, alkyl or aryl.

2.3 The history of metal complexes in bioinorganic studies

While the study of the coordination chemistry of thiosemicarbazones has long been of interest with the earliest review being published in 1974 (Chellan *et al*., 2010), in contrast medicinal inorganic chemistry has its origins in antiquity and the earliest

account of the use of metals for treating disease was found in Ebers Papyrus which dates to 1500 BC (Dabrowiak, 2012). This ancient event considered the first medical application that describes the use of copper for reducing inflammation and iron for treating anemia (Dabrowiak, 2012).

On the other hand according to Pelosi (2010), traces of interest in thiosemicarbazones date back to the beginning of the 20th century but the first reports on their medical utilization began to appear in the fifties as drugs against tuberculosis and leprosy. In the sixties their antiviral properties were discovered, and a huge amount of research was carried out that eventually led to the commercialization of methisazone (Marboran), which is a drug used to treat smallpox (Pelosi, 2010). Hence, today transition metal complexes of thiosemicarbazones are under intense study in search of lead compounds against different diseases such as Malaria.

2.4 The reaction mechanism of metal complexes of HL^1 and HL^2 ligands

In general, two geometrical isomers about the amine double bond (*E* and *Z*) are possible for the thiosemicarbazones, of which the *Z* isomer is stabilized by an intramolecular hydrogen bond between N(3)-H and the heterocyclic nitrogen (figure 4), (Pingaew, 2010)

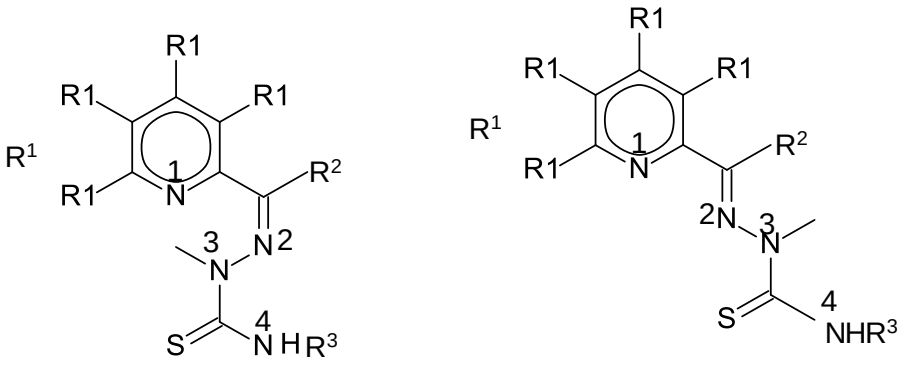

Figure 4: Structures of α-(N)-heterocyclic thiosemicarbazones: R1-R3 = hydrogen, alkyl group or aryl group; Z (left) and E (right) geometrical isomers (Pingaew, 2010)

There have been extensive reports on the synthesis of thiosemicarbazone complexes with metals including vanadium, zinc, cobalt, gold, nickel, silver, copper and iron (Chellan, 2010). With these metals varying the substituents of the carbon of thiosemicarbazone ligands influences their bonding mode to the metal (Chellan *et al*., 2010). For the foremost majority of cases the activity of the ligand is greatly enhanced by the presence of a metal ion (Pelosi, 2010). In support, Kumar *et al*., (2013) also believes that the biological activities of thiosemicarbazones are considered to be due to their ability to form chelates with metals (figure 5). As a result Huang *et al*. (2004) findings, indicated that biological essential life processes requiring metal (such as calcium, sodium and iron) usually involves enzymatic, structural or reactive roles and the catalytic activities for an estimated 12% of all enzymes can be ascribed to metal center. This is because the metals act to bridge substrate to enzymes such that electrons are withdrawn from the metal and the excess local positive charge lowers the free energy of enzyme activation (Huang *et. al*., 2004).

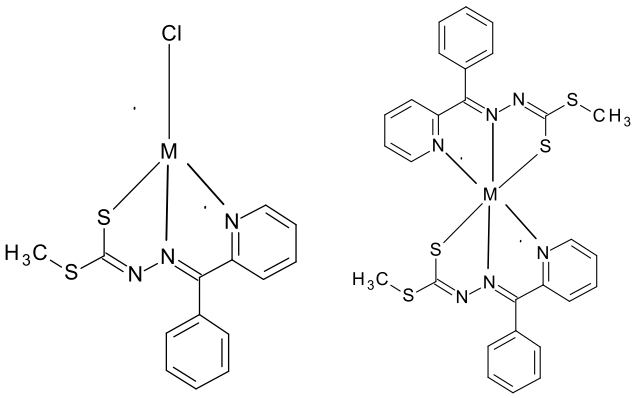

Figure 5: Possible binding sites of metal ions (M = Cu^{2+}, Zn^{2+}, Co^{2+}, Ni^{2+} and Fe^{2+}) to HL^1 and HL^2 in coordination of deprotonated ligands.

2.5 The known synthesized ligands (HL^1 and HL^2) and their corresponding metal complexes

2.5.1 The synthesis of 2-phenylpyridine S-methlydithiocarbazate (HL^1) and 2-pyridyl ketone S-methlydithiocarbazate (HL^2)

Although metal complexes of thiosemicarbazones ligands have been investigated extensively, less work has been reported on complexes of the related dithiocarbazates (Ali *et al*., 2011), According to literature Li *et al*. (2012), the preparation of 2-benzoylpyridine S-methyldithiocarbazates and 2-benzoylpyridine S-phenyldithiocarbazate was done by adding dropwise ethanol solution (15 mL) containing 2-benzoylpyridine (0.73 g, 4.0 mmol) to an ethanol solution (20 mL) of S-methyldithiocarbazate/S-phenyldithiocarbazate (0.49 g, 4.0 mmol) respectively with five drops of acetic acid as catalyst. After refluxed for 2 h, the resultant solution was vacuum filtered. Products separated were recrystallised from hot ethanol and dried over silica gel in vacuo, yielding 81% of 2-benzoylpyridine

S-methyldithiocarbazate (figure 6) and 76% 2-benzoylpyridine S-phenyldithiocarbazate.

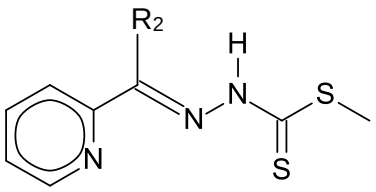

Figure 6: Structure of 2-benzoylpyridine S-methyldithiocarbazate (HL^1, R_2 = phenyl (Ph)) and 2-pyridyl ketone S-methlydithiocarbazate (HL^2, R_2 = pyridine).

Figure 6 above shows the derivative of the ligand that have been tested for microbial effects against selected bacteria, fungi and K562 leukaemia cell (Li *et al*., 2012), but they have not been tested for antimalaria activities. Ali *et al*. (2012) prepared 2-aminoacetophenone s-methyldithiocarbazate ligand by adding a solution of 20-aminoacetophenone (2.0 g; 0.0148 mol) in absolute ethanol (15 ml) to a boiling solution of S-methyldithiocarbazate (1.81 g; 0.0148 mol) in the same solvent (50 ml). Two drops of concentrated HCl were added and then the mixture was refluxed for ca. 3.5 h and cooled. The resulting crystals of the Schiff base were filtered off, washed with ethanol and later with diethyl ether. The yield obtained was 1.80 g (50%).

Also Hamid *et al*. (2009) prepared 2-Acetylpyrazine S-methyldithiocarbazate and 2-Acetylpyrazine S-benzyldithiocarbazate by adding 2-Acetylpyrazine (0.012 mol) in absolute ethanol (20 mL) to a solution of the appropriate S-methyldithiocarbazate and S-benzyldithiocarbazate (0.012 mol) in absolute ethanol (30 ml) respectively. The mixture was heated on a water bath for 10 min and left to stand overnight whereupon the compound that had formed was then filtered off, washed with diethyl ether and dried in a desiccator over anhydrous silica gel. The yields obtained were

94% 2-Acetylpyrazine s-methyldithiocarbazate and 94% for Acetylpyrazine S-benzyldithiocarbazate.

2.5.2. The synthesis and characterization of metal complexes of HL^1 and HL^2

There are lots of synthesized metal complexes of thiosemicarbazones derivatives in literature (Huang *et. al*., 2004). However these similar (to these under study) synthesized metal complexes of thiosemicarbazones has followed the standard published preparation procedures according to Hamid *et al.* (2009), who have done magnetic, spectroscopic and X-ray crystallographic structural studies of 2-acetylpyrazine S-methyldithiocarbazate and 2-acetylpyrazine S-benzyldithiocarbazate. Li *et al*. (2011) have prepared $[Cu_2(HL^1)_2(CH_3COOH)](ClO_4)$, $[Zn_2(HL^1)_2(ClO_4)]$ and $[Zn(HL^2)_2)$, where HL^1 and HL^2 are 2-benzoylpyridine S-methyldithiocarbazate and 2-benzoylpyridine S-phenyldithiocarbazate. During this event ethanol solution containing Cu^{2+} and Zn^{2+} ions was added to an ethanol solution of HL^1 and HL^2. The resulting reaction mixture was refluxed for 4 hours. The solid product formed was isolated and washed with ethanol. This crude product was further recrystallized from ethanol to yield green microcrystals in case of Cu and yellow microcrystal in case of Zn (Li *et al*., 2011). Also Lebano *et al*. (2013) conducted studies on synthesis, structures and spectroscopy of nickel (II) and cobalt (II) complexes with metal derivatives of N-substituted thiosemicarbazones.

2.5.3 Biological activities of metal complexes containing HL^1 and HL^2 ligands

Some metal complexes possess biological activities and according to Garoufis (2008), Pd (II) complexes of various donor atoms of thiosemicarbazone ligands possess anti-tumor and anti-viral activities. According to Arulmruga *et al*. (2010), transition metal complexes of Schiff base's ligands are important enzyme models compared to Schiff's base compounds themselves. Arulmruga *et al*. (2010) also cited that some synthesized transition (e.g Ni (II)) complexes with thiosemicarbazone Schiff bases derived from 2-formylindole, salicylaldehyde and N-amino rhodanine were characterized by elemental analysis, IR, Mass, ^{1}HNMR and electronic spectra (Arulmruga *et al*. 2010). Afterward the later were screened for antimicrobial activities against *Bacillus cerens, Escherichia coli, Pseudomonas aeruginosa, Staphylococcus aureus and Candida albicans* (Arulmruga *et al*. 2010). It results that ligands do not have any activity, where as their complexes showed more activity against the same organisms under identical experimental conditions (Arulmruga *et al*. 2010).

S-alkyl thiosemicarbazones (similar to s-methyl thiosemicarbazones ligand under study) and some of their Zn (II) and Pd (II) complexes, were investigated for their antimicrobial activity (Garoufis, 2008). These metal complexes were tested against bacteria such as *Escherichia coli*, *Klebsiella pneumoniae*, *Proteus mirabilis*, *Pseudomonas aeruginosa*, *Salmonella typhi*, *Shigella flexneri*, *Staphylococcus aureus*, *S. epidermidis*, and *Candida albicans* and they showed antibacterial and antifungal activities (Garoufis, 2008).

2.6 Statement of the research problem

Treatment and control of malaria have become more difficult due to lack of vaccines, spread of drug-resistant parasites and insecticide-resistant mosquitoes and therefore in order to control this disease new antimalarial drugs have to be developed (de Oliveira *et al*. 2007). Malaria is a major global health problem, with an estimated 300 to 500 million clinical cases occurring annually (Saifi *et al*., 2013). According to Alegana *et al*. (2013), in Namibia most health facilities with Malaria cases are located in Zambezi, Kavango West and East, Ohangwena, Oshana and Omusati regions where population density is greatest and statistically in total, 134 851 cases were clinically diagnosed while 90 835 individuals were examined for malaria parasites of which, 9 893 were positive in these regions. However the eradication of malaria continues to be frustrated by the continued looming threat of chloroquine resistant parasites which are poised to make malaria treatment even more expensive (Laufer *et al*., 2006). Hence, there is a need to search for a new and cheap lead compound using thiosemicarbazones and their derivatives. Thiosemicarbazones and their metal complexes provided new chemical entities which were investigated for potential anti-plasmodial activity.

2.7 The Aim of the study

The objectives of this research were as follows:

- ✓ to synthesize the 2-benzoylpyridine-s-methyldithiocarbazate (HL^1) and 2-dipyradylketone-s-methyldithiocarbazate (HL^2) ligands.

- ✓ to synthesize metal complexes from synthesized HL^1 and HL^2 ligands using copper (II), zinc (II), cadmium (II) and nickel (II), iron (II), silver (I), manganese (II), and cobalt (II) salts.
- ✓ to characterize the ligands and their metal complexes using EA, FT-IR and ^{1}HNMR.
- ✓ to perform biological evaluation against *Plasmodium falciparum* activities on the synthesized ligands and metal complexes.

2.8 Significance of the research

Despite that large amount of information are available on the synthesis and characterization of metal chelates derived from nitrogen-sulphur containing ligands, few are available for the application of them toward antiplasmodial activity, this research is of great interest because the ligands; 2-benzoylpyridine-*s*-methyldithiocarbazate (HL^1) and di-2-pyradylketone-*s*-methyldithiocarbazate (HL^2) and their corresponding metal complexes: (copper (II), zinc (II), cadmium (II) and Nickel (II), iron (II) and cobalt (II) were synthesized using the method of acid catalyzed condensation reaction. Moreover, this research has adopted the synthesis of a new system (s-methyldithiocarbazate with schiff's base ligands of 2-benzoylpyridine and di-2-pyridylketone) to determine if it provides new chemical entities of antiplasmodial.

CHAPTER 3: MATERIALS AND METHODS

3.1 Apparatus, chemicals and general techniques

All solvents and reagents tabulated in Table 1 were procured from Aldrich Chemical Company and they were used without any further purification.

Table 1: The characterization of main starting reagents

Starting compounds	Colour	Molecular formula	Molecular Weight (g/mol)
S-methyldithiocarbazate	Light green	$C_2H_6N_2S_2$	122.21
2-Benzoyl pyridine	colourless	$C_{12}H_9NO$	183.21
di-2-pyridyl ketone	colourless	$C_{11}H_8N_2O$	184.20
Copper(II) chloride dihydrate	Turquoise	$CuCl_2.6H_2O$	170.48
Iron(II) chloride tetrahydrate	Pale green	$FeCl_2.4H_2O$	198.81
Nickel(II)chloride hexahydrate	Green	$NiCl_2.6H_2O$	237.70
Cadmium(II) chloride hydrate	White	$CdCl_2.H_2O$	183.32
Zinc(II) Chloride	colourless	$ZnCl_2$	136.28
Cobalt(II) chloride hexahydrate	Red	$CoCl_2.6H_2O$	237.93

Elemental analysis for C, H and N were carried out using a Perkin-Elmer 240 analyzer using acetanilide as a reference compound. The melting points were determined with the melting point electrically heated apparatus. The IR spectra were recorded using FT-IR spectrometer. ^{1}HNMR spectra were recorded on Bruker AV spectrometer at 300 MHz in D-6 DMSO with TMS as the internal reference.

3.2 The synthesis of thiosemicarbazone ligands

3.2.1 The synthesis of 2-benzoylpyridine-*s*-methyldithiocarbazate (HL^1) ligand

The 2-benzoylpyridine-*s*-methyldithiocarbazate (HL^1) ligand (scheme 2) was prepared by adding drop-wise ethanol (25 ml) solution containing 2-benzoylpyridine (0.54 g, 7.30 mmol) to an ethanol solution (25 ml) containing equimolar quantities of *s*-methyldithiocarbazate (0.33 g, 2.73 mmol) with 3 drops of acetic acid as a catalyst. The reaction mixture was refluxed for 3 hours and thereafter it was refrigerated at 4 ˚C for 24 hours. The resultant solution was filtered to precipitate finely yellow powder which was washed with 15 ml of double distilled water followed by 10 ml of ethanol and later 10 ml of diethyl ether. The precipitate was dried on a vacuum pump for 35 minutes, weighed on analytical balance. Yield: 48%; m.p. 116 – 118 °C. Anal. Cal. for $C_{14}H_{13}N_3S_2$ (%): C, 58.5; H, 4.6; N, 14.6. Found: C, 58.59; H, 4.90; N, 15.87%. Selected IR data (ν, cm^{-1}): ν(N-H) 3400w,b; ν(C-H), 3210w; ν(C=N) + ν(C=C), 1425s, 1400s; ν(N-N), 1225m; ν(C-N) + ν(C=S), 1100s, 1050s; ν(Py), 690s. ^{1}HNMR (600 MHz, DMSO-d_6, ppm, δ): 14.4 (m, 1H, N^2-H), 3.31 (s, 3H, C^1-H_3), 7.50 (s, 5H, phenyl: $C^{7\text{-}11}$-H), 8.18 (s, 2H, Py: $C^{4\text{-}5}$-H), 8.50 (m, 1H, C^6-H), 8.85 (m, 1H, C^3-H). The reaction scheme of 2-benzoylpyridine-*s*-methyldithiocarbazate (HL^1 ligand) is shown below by scheme 2.

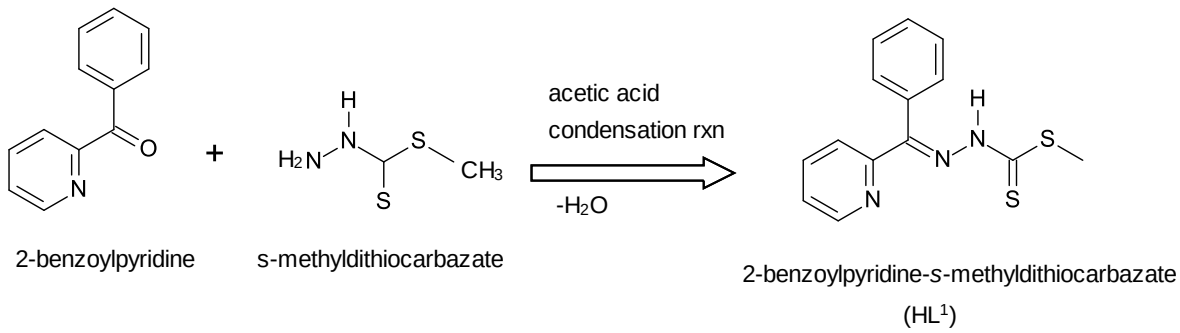

Scheme 2: The synthesis of HL^1 ligand

3.2.2 The synthesis of di-2-pyridyl ketone-s-methyldithiocarbazate (HL^2) ligand

The synthesis of 2-dipyridyl ketone-s-methyldithiocarbazate (HL^2) ligand was prepared by adding drop-wise ethanol (25 ml) solution containing 2-dipyridyl ketone (1.02 g, 1.36 mmol) to an ethanol solution (25 ml) containing equimolar quantities of *s*-methyldithiocarbazate (0.67 g, 1.36 mmol) with 3 drops of acetic acid as a catalyst. The reaction mixture was refluxed for 3 hours and thereafter it was refrigerated at 4 ˚C for 24 hours. The resultant solution was filtered to precipitate fluffy yellow precipitates which was washed with 15 ml of double distilled water followed by 10 ml of ethanol and later 10 ml of diethyl ether. The precipitate was dried on a vacuum pump for 35 minutes and weighed on analytical balance. Yield: 69%; m.p. 158 – 159 ℃. Anal. Cal. for $C_{13}H_{12}N_4S_2$ (%): C, 54.1; H, 4.2; N, 19.4. Found: C, 54.14; H, 4.36; N, 21.12%. Selected IR data (ν, cm^{-1}): ν(N-H) 3615w; ν(C-H), 3000w; ν(C=N) + ν(C=C), 1425s, 1400s; ν(N-N), 1250m; ν(C-N) + ν(C=S), 1025s, 1000s; ν(Py), 689s. ^{1}HNMR (600 MHz, DMSO-d_6, ppm, δ): 15.11 (m, 1H, N^2-H), 3.31 (s, 3H, C^1-H_3), 8.85 (s, 2H, Py: C^3-H and C^{10}-H), 8.65 (s, 2H, Py: C^6-H and C^7-H), 8.00(s, 2H, Py: C^4-H and C^9-H), 7.65 (s, 2H, Py: C^5-H and C^8-H). The reaction scheme for

the synthesis of di-2-pyridyl ketone-s-methyldithiocarbazate (HL^2 ligand) is shown below by scheme 3.

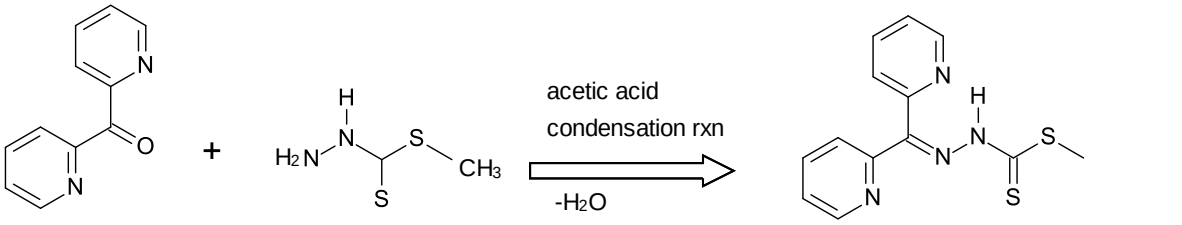

Scheme 3: The synthesis of HL^2 ligand

3.3 The synthesis of metal complexes from some transition metal ions with thiosemicarbazone ligands (HL^1 and HL^2)

3.3.1 The synthesis of Fe-2-benzoylpyridine-*s*-methyldithiocarbazate (FeL^1_2) complex from Fe^{2+} with HL^1 ligand.

FeL^1 was prepared by adding drop-wise aqueous solution (10 ml) containing $FeCl_2.4H_2O$ (0.35 g, 1.74 mmol) to a hot ethanol solution (25 ml) of HL^1 ligand (1.00 g, 3.48 mmol) while stirring at the same time. The solid products formed were isolated from the solution by vacuum filtration, washed with double distilled water (10 ml), ethanol (10 ml) and diethyl ether (15 ml). The resultant green crude precipitate was dried on a vacuum pump for 45 minutes. Yield: 92%; m.p. 249 – 286°C. Anal. Cal. for $C_{28}H_{24}FeN_6S_4$ (%): C, 53.5; H, 3.8; N, 13.4. Found: C, 53.57; H, 4.27; N, 14.18%. Selected IR data (ν, cm^{-1}): ν(N-H) 3400w; ν(C-H), 3050w; ν(C=N) + ν(C=C), 1400s; ν(N-N), 1325s; ν(C-N) + ν(C=S), 1050s; ν(C-S) 1140w;

v(Py), 650w. ^{1}HNMR (600 MHz, DMSO-d_6, ppm, δ): 3.31 (s, 3H, C^{1}-H_3), 7.50 (s, 5H, phenyl: C^{7-11}-H), 8.18 (s, 2H, Py: C^{4-5}-H), 8.50 (m, 1H, C^{6}-H), 8.85 (m, 1H, C^{3}-H). The schematic synthesis of FeL^{1} complex is shown in scheme 4.

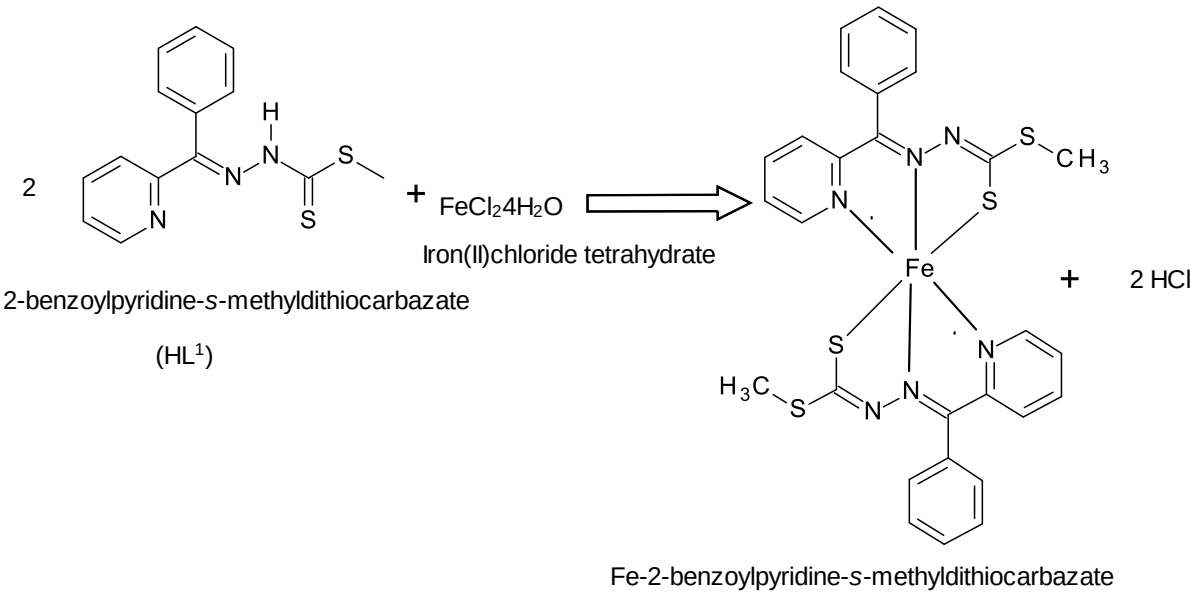

Scheme 4: The synthesis of FeL^{1}_{2} complex

3.3.2 The synthesis of Co-chloride-2-benzoylpyridine-*s*-methyldithiocarbazate ($CoL^{1}Cl$) complex from Co^{2+} with HL^{1} ligand.

CoL^{1} was prepared by adding drop-wise aqueous solution (10 ml) containing $CoCl_2.6H_2O$ (0.416 g, 1.74 mmol), to a hot ethanol solution (25 ml) of HL^{1} ligand (1.00 g, 3.48 mmol) while stirring at the same time. The solid products formed were isolated from the solution by vacuum filtration, washed with double distilled water (10 ml), ethanol (10 ml) and diethyl ether (15 ml). The resultant brown crude precipitate was dried on a vacuum pump for 60 minutes. Yield: 59%; m.p. 281-288°C. Anal. Cal. for $C_{14}H_{12}ClCoN_3S_2$ (%): C, 44.2; H, 3.2; N, 11.0. Found: C,

46.22; H, 3.38; N, 11.37%. Selected IR data (ν, cm^{-1}): ν(N-H) 3500w; ν(C-H), 3050w; ν(C=N) + ν(C=C), 1400s; ν(N-N), 1350m; ν(C-N) + ν(C=S), 1000s; ν(C-S) 1125s; ν(Py), 650s. ^{1}HNMR (600 MHz, DMSO-d_6, ppm, δ): 3.28 (s, 3H, C^1-H_3), 7.72 (s, 5H, phenyl: $C^{7\text{-}11}$-H), 8.00 (s, 2H, Py: $C^{4\text{-}5}$-H), 7.92 (m, 1H, C^6-H), 8.12 (m, 1H, C^3-H). The schematic synthesis of CoL^1Cl complex is shown in scheme 5.

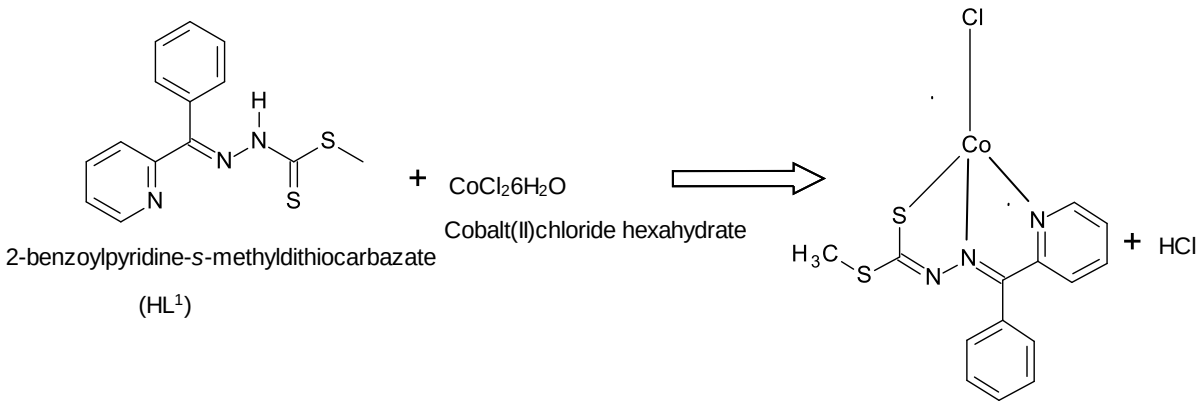

2-benzoylpyridine-*s*-methyldithiocarbazate (HL^1)

Co-chloride-2-benzoylpyridine-*s*-methyldithiocarbazate

Scheme 5: The synthesis of CoL^1Cl complex

3.3.3 The synthesis of Cu-chloride-2-benzoylpyridine-*s*-methyldithiocarbazate (CuL^1Cl) complex from Cu^{2+} with HL^1 ligand

The CuL^1Cl was prepared by adding drop-wise aqueous solution (10 ml) containing $CuCl_2$ (0.148 g, 0.870 mmol) to a hot ethanol solution (25 ml) of HL^1 ligand (0.500 g, 1.74 mmol) with constant stirring. The solid product formed was isolated from the solution by vacuum filtration, washed with double distilled water (10 ml), ethanol (10 ml) and diethyl ether (15 ml). The crude green precipitate was dried on a vacuum pump for 35 minutes. Yield: 51%; m.p. 228 – 232°C. Anal. Cal. for $C_{14}H_{12}ClCuN_3S_2$ (%): C, 43.6; H, 3.1; N, 10.9. Found: C, 46.30; H, 3.27; N, 12.427%. ^{1}HNMR (600

MHz, DMSO-d_6, ppm, δ): 3.27 (s, 3H, C^1-H_3), 7.00 (s, b, 5H, phenyl: $C^{7\text{-}11}$-H), 8.71 (s, 2H, Py: $C^{4\text{-}5}$-H), 9.43 (m, b, 1H, C^6-H), 10.35 (w, b, 1H, C^3-H). The schematic synthesis of CuL^1Cl complex is shown below in scheme 6.

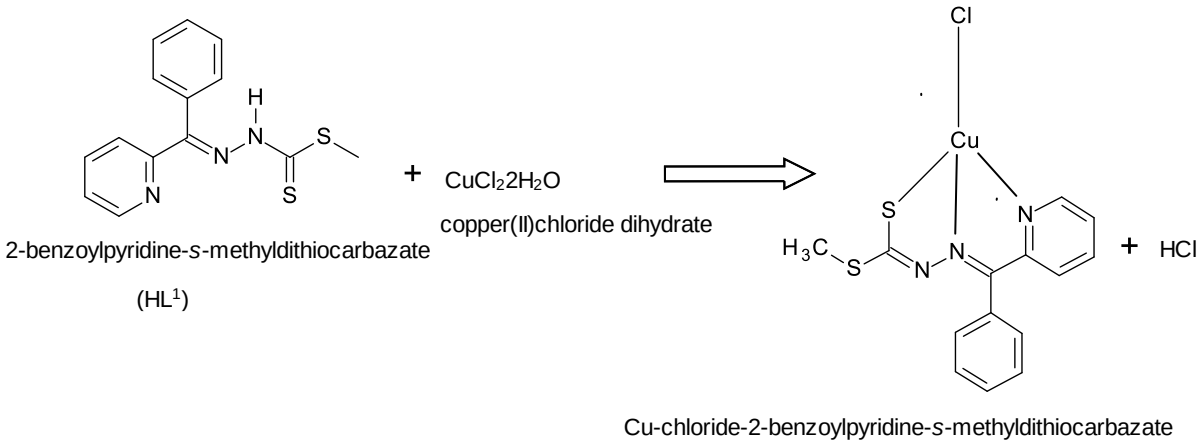

2-benzoylpyridine-*s*-methyldithiocarbazate

(HL^1)

Cu-chloride-2-benzoylpyridine-*s*-methyldithiocarbazate

Scheme 6: The synthesis of CuL^1Cl complex

3.3.4 The synthesis of Cu-chloride-di-2-pyridylketone-*s*-methyldithiocarbazate (CuL^2Cl) complex from Cu^{2+} with HL^2 ligand

The CuL^2Cl complex was prepared by adding drop-wise aqueous solution (10 ml) containing $CuCl_2$ (0.305 g, 0.867 mmol) to a hot ethanol solution (25 ml) of HL^2 ligand (0.500 g, 1.73 mmol) with constant stirring. The leafy green solid product formed was isolated from the solution by vacuum filtration, washed with double distilled water (10 ml), ethanol (10 ml) and diethyl ether (15 ml). The crude green precipitate was dried on a vacuum pump for 35 minutes. Yield: 46%; m.p. 235 – 240°C. Anal. Cal. for $C_{13}H_{11}ClCuN_4S_2$ (%): C, 40.4; H, 2.9; N, 14.5. Found: C, 40.58; H, 2.91; N, 15.03%. Selected IR data (ν, cm^{-1}): ν(N-H) 3450w; ν(C=N) + ν(C=C), 1400s; ν(N-N), 1350m; ν(C-N) + ν(C=S), 1000s; ν(C-S), 1100S; ν(Py),

650m. ^{1}HNMR (600 MHz, DMSO-d_6, ppm, δ): 3.31 (s, 3H, C^{1}-H_3), 10.06 (s, 2H, Py: C^{3}-H and C^{10}-H), 8.77 (s, 2H, Py: C^{6}-H and C^{7}-H), 8.61(s, 2H, Py: C^{4}-H and C^{9}-H), 7.51 (s, 2H, Py: C^{5}-H and C^{8}-H). The schematic synthesis of $CuL^{2}Cl$ complex is shown below in scheme 7.

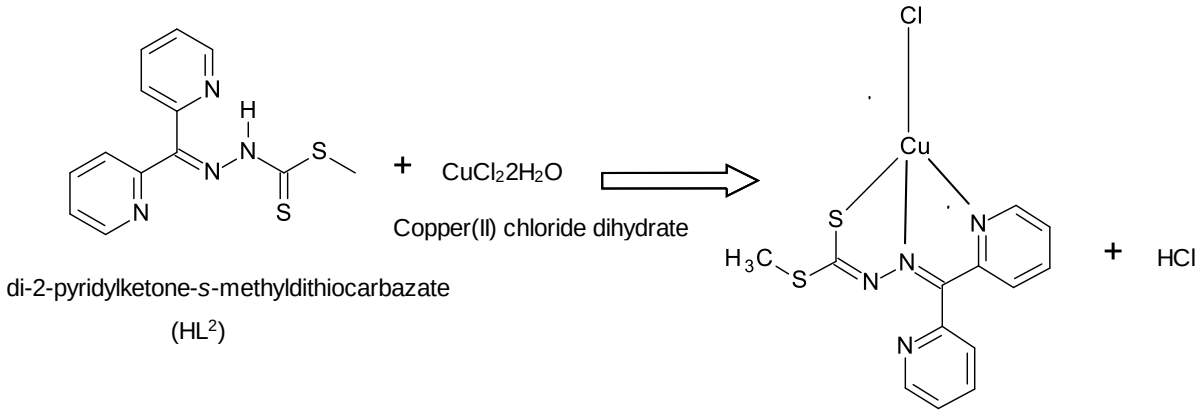

di-2-pyridylketone-*s*-methyldithiocarbazate

(HL^{2})

Cu-chloride-di-2-pyridylketone-*s*-methyldithiocarbazate

Scheme 7: The synthesis of $CuL^{2}Cl$ complex

3.3.5 The synthesis of Ni-2-benzoylpyridine-*s*-methyldithiocarbazate (NiL^{1}_{2}) complex from Ni^{2+} with HL^{1} ligand

A solution of $NiCl_2 6H_2O$ (0.208 g, 8.69 mmol) dissolved in water (10 ml) was added drop-wise with constant stirring to a hot ethanol solution (25 ml) of HL^{1} ligand (0.504 g, 1.74 mmol). The brown solid product formed was isolated from the solution by vacuum filtration, washed with double distilled water (10 ml), ethanol (10 ml) and diethyl ether (15 ml). The resultant brown crude precipitate was dried on a vacuum pump for 45 minutes. Yield: 92%; m.p. 270 – 282℃. Anal. Cal. for $C_{28}H_{24}NiN_6S_4$ (%): C, 53.3; H, 3.8; N, 13.3. Found: C, 53.42; H, 4.14; N, 13.92%. Selected IR data (ν, cm^{-1}): ν(C-H), 3100w; ν(C=N) + ν(C=C), 1400s, 1425w; ν(C-N)

+ ν(C=S), 1000m; ν(C-S) 1100s; ν(Py), 650w. ^{1}HNMR (600 MHz, DMSO-d_6, ppm, δ): 3.20 (s, 3H, C^1-H_3), 7.90 (s, b, 5H, phenyl: $C^{7\text{-}11}$-H), 9.0 (s, b, 2H, Py: $C^{4\text{-}5}$-H), 8.50 (m, b, 1H, C^6-H), 12.30 (m, b, 1H, C^3-H). The schematic synthesis of $NiL^1{}_2$ complex is shown in scheme 8.

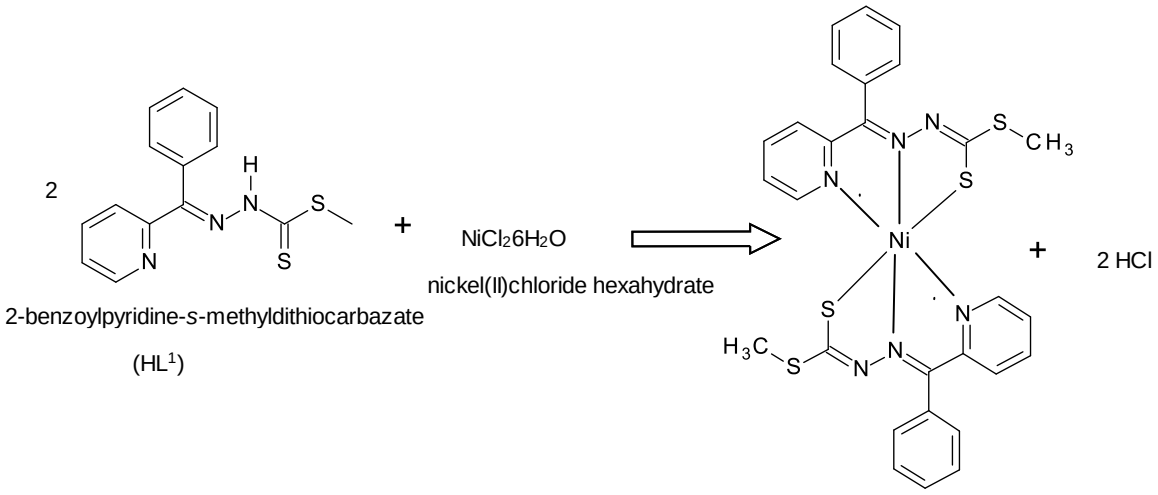

Scheme 8: The synthesis of $NiL^1{}_2$ complex

3.3.6 The synthesis of Ni-di-2-pyridylketone-s-methyldithiocarbazate ($NiL^2{}_2$) complex from Ni^{2+} and HL^2 ligand

A solution of $NiCl_26H_2O$ (0.42 g, 1.74 mmol) dissolved in water (10 ml) was added drop-wise with constant stirring to a hot ethanol solution (25 ml) of HL^2 ligand (1.00 g, 3.74 mmol). The brown solid product formed was isolated from the solution by vacuum filtration, washed with double distilled water (10 ml), ethanol (10 ml) and diethyl ether (15 ml). The resultant brown crude precipitate was dried on a vacuum pump for 45 minutes. Yield: 69%; m.p. 271 – 288°C. Anal. Cal. for $C_{26}H_{22}N_8NiS_4$ (%): C, 49.3; H, 3.5; N, 17.7. Found: C, 49.46; H, 3.66; N, 18.71%. Selected IR data

(ν, cm^{-1}): ν(N-H) 3625w; ν(C-H), 3050w; ν(C=N) + ν(C=C), 1425m, 1400s; ν(N-N), 1300m; ν(C-N) + ν(C=S), 1000s; ν(C-S), 1100s. ^{1}HNMR (600 MHz, DMSO-d_6, ppm, δ): 3.31 (s, 3H, C^1-H_3), 12.25 (m, b, 2H, Py: C^3-H and C^{10}-H), 10.12 (s, b, 2H, Py: C^6-H and C^7-H), 8.66 (s, b, 2H, Py: C^4-H and C^9-H), 8.42 (s, b, 2H, Py: C^5-H and C^8-H). The reaction scheme of NiL^2_2 complex is shown in scheme 9.

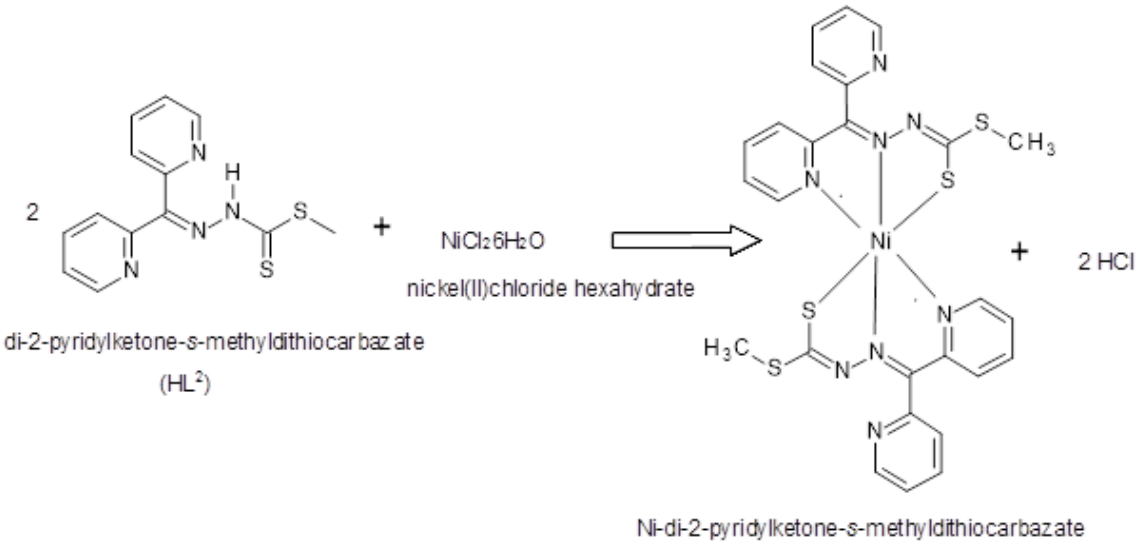

Scheme 9: The synthesis of NiL^2_2 complex

3.3.7 The synthesis of Cd-2-benzoylpyridine-*s*-methyldithiocarbazate (CdL^1_2) complex from Cd^{2+} with HL^1 ligand

A solution of $CdCl_2H_2O$ (0.505 g, 0.869 mmol) dissolved in water (10 ml) was added drop-wise with constant stirring to a hot ethanol solution (25 ml) of HL^1 ligand (0.505 g, 1.74 mmol). The yellow solid product formed was isolated from the solution by vacuum filtration, washed with double distilled water (10 ml), ethanol (10 ml) and diethyl ether (15 ml). The resultant powdery yellow crude precipitate was dried on a vacuum pump for 45 minutes. Yield: 41%; m.p. 240 – 259°C. Anal.

Cal. for $C_{28}H_{24}CdN_6S_4$ (%): C, 49.1; H, 3.5; N, 12.3. Found: C, 50.12; H, 3.66; N, 15.28%. Selected IR data (ν, cm^{-1}): ν(N-H), 3400w; ν(C-H), 3150w; ν(C=N) + ν(C=C), 1400s, 1600w; ν(N-N), 1300m; ν(C-N) + ν(C=S), 1000m; ν(C-S) 1148s; ν(Py), 650w. ^{1}HNMR (600 MHz, DMSO-d_6, ppm, δ): 3.27 (s, 3H, C^1-H_3), 7.50 (s, 5H, phenyl: $C^{7\text{-}11}$-H), 7.62 (s, 2H, Py: $C^{4\text{-}5}$-H), 8.0 (s, 1H, C^6-H), 8.25 (m, 1H, C^3-H). The schematic synthesis of $CdL^1{}_2$ complex is shown in scheme 10.

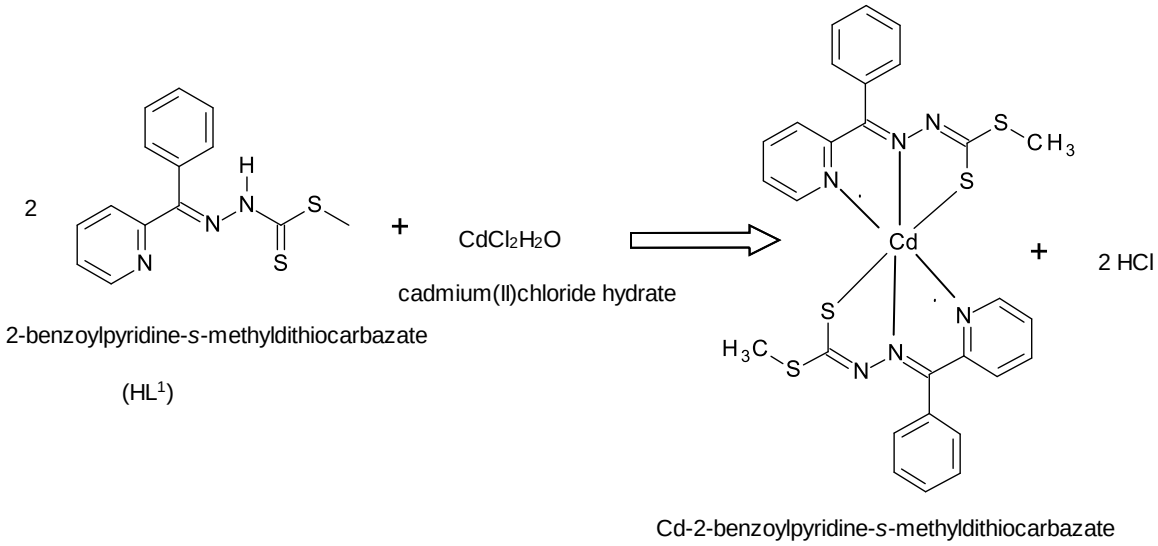

Scheme 10: The synthesis of $CdL^1{}_2$ complex

3.3.8 The synthesis of Cd-chloride-di-2-pyridylketone-s-methyldithiocarbazate (CdL^2Cl) complex from Cd^{2+} with HL^2 ligand

The CdL^2Cl complex was prepared by adding drop-wise aqueous solution (10 ml) containing $CdCl_2H_2O$ (0.321 g, 1.73 mmol) to a hot ethanol solution (25 ml) of HL^2 ligand (1 g, 3.47 mmol) with constant stirring. The yellow solid product formed was isolated from the solution by vacuum filtration, washed with double distilled water

(10 ml), ethanol (10 ml) and diethyl ether (15 ml). The crude yellow precipitate was dried on a vacuum pump for 35 minutes. Yield: 81%; m.p. 257 – 262°C. Anal. Cal. for $C_{13}H_{11}ClCdN_4S_2$ (%): C, 35.9; H, 2.5; N, 12.9. Found: C, 35.98; H, 2.65; N, 13.40%. Selected IR data (ν, cm^{-1}): ν(N-H) 3600w; ν(C-H), 3100w; ν(C=N) + ν(C=C), 1400s; ν(N-N), 1300s, 1250m; ν(C-N) + ν(C=S), 950s; ν(C-S), 1100s; ν(Py), 650m. ^{1}HNMR (600 MHz, DMSO-d_6, ppm, δ): 3.31 (s, 3H, C^1-H_3), 8.78 (s, 2H, Py: C^3-H and C^{10}-H), 8.25 (s, 2H, Py: C^6-H and C^7-H), 8.00 (s, 2H, Py: C^4-H and C^9-H), 7.55 (s, 2H, Py: C^5-H and C^8-H). The schematic synthesis of CdL^2Cl complex is shown below in scheme 11.

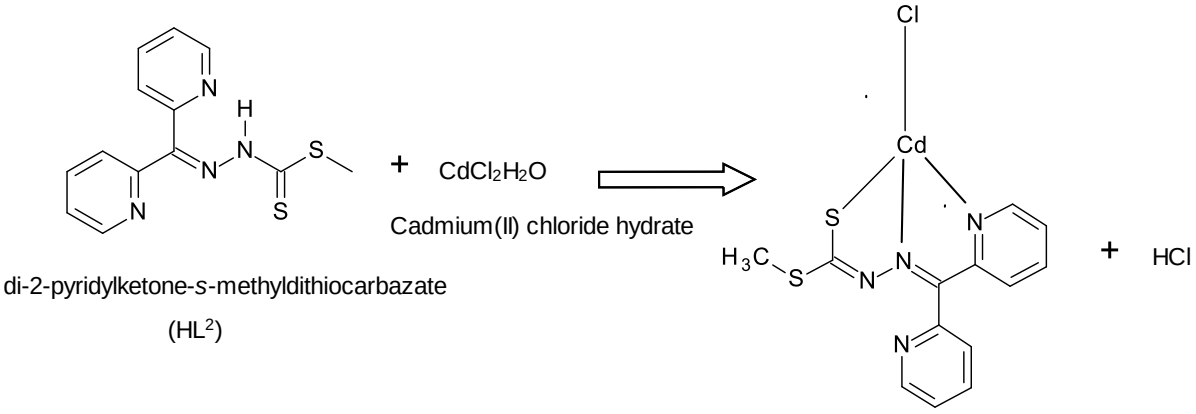

di-2-pyridylketone-*s*-methyldithiocarbazate

(HL^2)

Cd-chloride-di-2-pyridylketone-*s*-methyldithiocarbazate

Scheme 11: The synthesis of CdL^2Cl complex

3.3.9 The synthesis of Zn-2-benzoylpyridine-*s*-methyldithiocarbazate (ZnL^1_2) complex from Zn^{2+} with HL^1 ligand

A solution of $ZnCl_2$ (0.121 g, 0.869 mmol) dissolved in aqueous (10 ml) was added drop-wise with constant stirring to a hot ethanol solution (25 ml) of HL^1 ligand (0.508 g, 1.74 mmol). The yellow solid product formed was isolated from the solution by vacuum filtration, washed with double distilled water (10 ml), ethanol (10 ml) and diethyl ether (15 ml). The resultant yellow crude precipitate was dried on a vacuum pump for 45 minutes. Yield: 63%; m.p. 269 – 274℃. Anal. Cal. for $C_{28}H_{24}ZnN_6S_4$ (%): C, 40.2; H, 2.9; N, 14.4. Found: C, 40.33; H, 2.84; N, 14.97%. ^{1}HNMR (600 MHz, DMSO-d_6, ppm, δ): 3.27 (s, 3H, C^1-H_3), 7.50 (s, 5H, phenyl: $C^{7\text{-}11}$-H), 7.61 (s, 2H, Py: $C^{4\text{-}5}$-H), 8.0 (s, 1H, C^6-H), 8.20 (m, 1H, C^3-H). The schematic synthesis of ZnL^1_2 complex is shown in scheme 11.

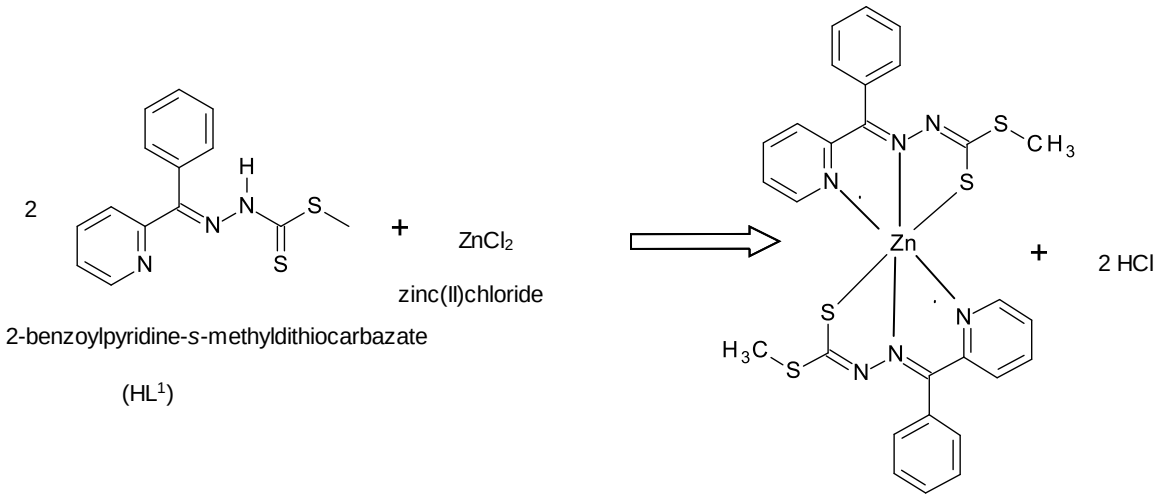

Scheme 12: The synthesis of ZnL^1_2 complex

3.3.10 The synthesis of Zn-chloride-di-2-dipyridylketone-s-methyldithiocarbazate (ZnL^2Cl) complex from Zn^{2+} with HL^2 ligand

The ZnL^2Cl complex was prepared by adding drop-wise aqueous solution (10 ml) containing $ZnCl_2$ (0.241 g, 1.73 mmol) to a hot ethanol solution (25 ml) of HL^2 ligand (1 g, 3.47 mmol) with constant stirring. The yellow solid product formed was isolated from the solution by vacuum filtration, washed with double distilled water (10 ml), ethanol (10 ml) and diethyl ether (15 ml). The crude yellow precipitate was dried on a vacuum pump for 45 minutes. Yield: 45%; m.p. 305 – 313°C. Anal. Cal. for $C_{13}H_{11}ClN_4S_2Zn$ (%): C, 40.2; H, 2.9; N, 14.4. Found: C, 40.33; H, 2.84; N, 14.97%. Selected IR data (ν, cm^{-1}): ν(N-H) 3600w; ν(C-H), 3100w; ν(C=N) + ν(C=C), 1400s; ν(N-N), 1300s, 1250m; ν(C-N) + ν(C=S), 950s; ν(C-S), 1100s; ν(Py), 650m. ^{1}HNMR (600 MHz, DMSO-d_6, ppm, δ): 3.31 (s, 3H, C^1-H_3), 8.75 (s, 2H, Py: C^3-H and C^{10}-H), 8.25 (s, 2H, Py: C^6-H and C^7-H), 7.55 (s, 2H, Py: C^4-H and C^9-H), 7.35 (s, 2H, Py: C^5-H and C^8-H). The schematic synthesis of ZnL^2Cl complex is shown below in scheme 13.

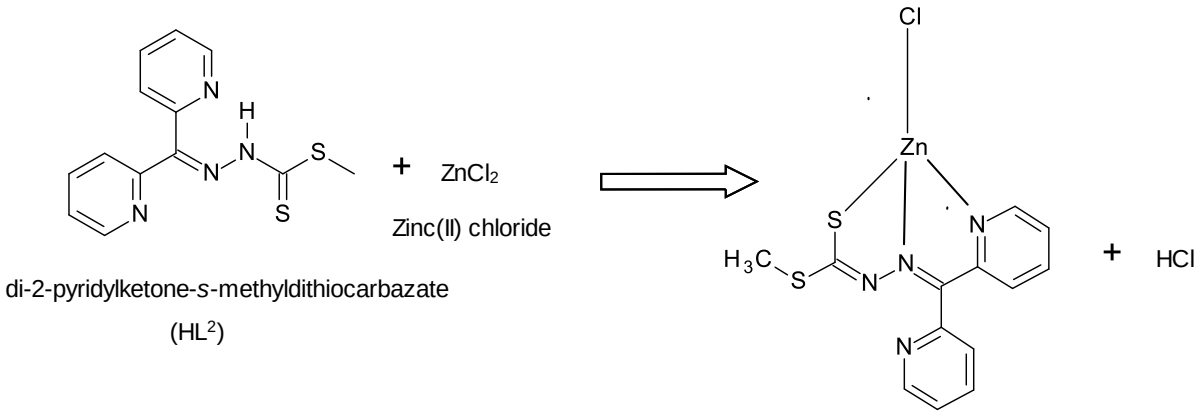

Scheme 13: The synthesis of ZnL^2Cl complex

3.4 The recrystallization of ligands and corresponding metal complexes for purity

Ligands and their corresponding metal complexes were recrystallized by dissolving them in a hot ethanol solution. Ethanol was chosen as the best solvent because it slightly dissolved the ligands (HL^1 and HL^2) at room temperature and completely dissolved them after heating. The hot solution was allowed to cool for 30 minutes and the precipitates were filtered off by vacuum filtration. The samples were further sent to university of Cape Town for elemental analysis and proton-NMR, which is a technique that characterize organic molecules in view of establishing their identity.

CHAPTER 4: RESULTS AND DISCUSSION

4.1 The physical properties of the synthesized ligands and metal complexes

HL^1 and HL^2 were prepared successfully by acid catalyzed condensation reaction with a reaction molar ratio of a 1:1 ketone to *s*-methyldithiocarbazate. In the presence of acetic acid, both HL^1 and HL^2 were prepared by a condensation reaction of s-methyldithiocarbazate with 2-benzoylpyridine and di-2-pyridylketone respectively. Analytical and physical data of the synthesized ligands are showed in Table 2.

4.1.1. Colour and percentage yield of the synthesized compounds

The reaction between s-methyldithiocarbazate with 2-benzoylpyridine ketone produced shinny yellow powder dithiocarbazate ligand (HL^1) with the molecular formula $C_{14}H_{13}N_3S_2$ (Mw: 287.40). The yield of this ligand was 48% when equimolar amount of reactants were used. Moreover, the reaction between s-methyldithiocarbazate with di-2-pyridyl ketone gave rise to a fluffy yellow HL^2 ligand with the molecular formula $C_{13}H_{12}N_4S_2$ (Mw: 288.39 g/mol) and a percentage yield of 69 %.

Metal complexes of HL^1 and HL^2 ligands were successfully synthesized, yielding different percentages. Metals such as Fe^{2+}, Ni^{2+}, Cd^{2+}, Cu^{2+} and Zn^{2+} gave a higher yield compared to that of Co^{2+}. Moreover, metal complexes were appearing different in color as compared to their corresponding parental ligands, and this confirmed that new different metal compounds are formed.

Table 2: The physicochemical characteristics, melting point and elemental analysis of the synthesized ligands and their metal complexes

Compound	Colour	Melting point, range (°C)	Elemental analysis, %found (%calculated)			Formula
			C	H	N	
HL^1	Crystal yellow	114 - 116	58.59 (58.5)	4.90 (4.6)	15.87 (14.6)	$C_{14}H_{13}N_3S_2$
HL^2	Fluffy yellow	154 - 158	54.14 (54.1)	4.36 (4.2)	21.12 (19.4)	$C_{13}H_{12}N_4S_2$
$FeL^1{}_2$	Dark green	249 - 286	53.57 (53.5)	4.27 (3.8)	14.18 (13.4)	$C_{28}H_{24}FeN_6S_4$
CoL^1Cl	Finely brown	281 - 288	46.22 (44.2)	3.38 (3.2)	11.37 (11.0)	$C_{14}H_{12}ClCoN_3S_2$
CuL^1Cl	Finely leafy green	228 - 232	46.30 (43.6)	3.27 (3.1)	12.42 (10.9)	$C_{14}H_{12}ClCuN_3S_2$
$NiL^1{}_2$	Crystal brown	270 - 282	53.42 (53.3)	4.14 (3.8)	13.92 (13.3)	$C_{28}H_{24}NiN_6S_4$
$ZnL^1{}_2$	Powderly yellow	269 - 274	52.94 (52.7)	4.08 (3.8)	16.11 (13.2)	$C_{28}H_{24}ZnN_6S_4$
$CdL^1{}_2$	Powderly yellow	240 - 259	50.12 (49.1)	3.66 (3.5)	15.28 (12.3)	$C_{28}H_{24}CdN_6S_4$
CuL^2Cl	Finely leafy green	235 - 240	40.58 (40.4)	2.91 (2.9)	15.03 (14.5)	$C_{13}H_{11}ClCuN_4S_2$
ZnL^2Cl	Powderly yellow	305 - 313	40.33 (40.2)	2.84 (2.9)	14.97 (14.4)	$C_{13}H_{11}ClN_4S_2Zn$
$NiL^2{}_2$	Crystal brown	271 - 288	49.46 (49.3)	3.66 (3.5)	18.71 (17.7)	$C_{26}H_{22}N_8NiS_4$
CdL^2Cl	Powderly yellow	257 - 262	35.98 (35.9)	2.65 (2.5)	13.40 (12.9)	$C_{13}H_{11}ClCdN_4S_2$

4.1.2 Melting point

The melting points of the synthesized ligands and their corresponding metal complexes are also shown in Table 2 above. HL^1 ligand was found to have a low melting point compared to its corresponding metal complexes and counterpart HL^2. The melting point of HL^2 ligand is lower than that of its corresponding metal complexes. The difference in melting point between the ligands and the complexes further prove that new compounds are formed that are different from their parental ligands. Moreover, lower melting point of ligand than their respective complexes shows that complexation increases the intra-atomic bonding effect of particles of these compounds (Daniel, 2009; Kiremire, 2010). Metal complexes of HL^1 ligand are also observed to melt at lower temperature in comparison to those of HL^2 and this could be due to an influence of melting points of individual ligands on such metal ions.

4.1.3 The solubility Test

Solubility test of all the synthesized ligands and metal complexes was done to determine the suitable solvents for compounds' recrystallization to purify them (table 3). None of the synthesized ligands and metal complexes was soluble in water, indicating that these compounds have low polarity. Copper complexes of both ligands were the only compounds which are partially soluble in methanol. Diethyl ether dissolved both ligands and almost every metal complex expect for $NiL^1{}_2$ and ZnL^2Cl complexes. Both ligands and metal complexes are extremely soluble in dimethylsulphoxide (DMSO) and dimethylformamide (DMF) with exception to CoL^1Cl complex which was just soluble. Acetone partially dissolved both ligands at

room temperature and failed to dissolve any of the synthesized metal complexes of both ligands. The solubility test proved that all the synthesized compounds to be stable in air and moisture. The color of the respective solvents remained the same, regardless the time the solid compounds were kept in such solvent confirming that these compounds remain intact and they do not decompose in most organic solvents. Different in solubility of each individual ligand and complex further proved that synthesized complexes are different from their parental ligands. Ethanol was chosen as suitable solvent because it slightly dissolved the ligands (HL^1 and HL^2) at room temperature and completely dissolved them after heating.

Table 3: The solubility tests of the HL^1, HL^2 and their metal complexes

	Solvents							
Compounds	**H_2O**	**MeOH**	**EtOH**	**Acetone**	**Et_2O**	**$CHCl_3$**	**DMSO**	**DMF**
HL^1	-	-	+	+	+++	++++	++++	++++
HL^2	-	-	+	+	+++	++++	++++	++++
FeL^1_2	-	-	-	-	+	+++	++	++++
CoL^1Cl	-	-	-	-	+	+++	++	++
CuL^1Cl	-	+	-	-	++	++++	++++	++++
NiL^1_2	-	-	-	-	-	++++	++++	++++
ZnL^1_2	-	-	-	-	+	+++	++++	++++
CdL^1_2	-	-	-	-	+	++++	++++	++++
CuL^2Cl	-	+	-	-	+	++++	++++	++++
ZnL^2Cl	-	-	-	-	-	++++	++++	++++
NiL^2_2	-	-	-	-	+	++++	++++	++++
CdL^2Cl	-	-	-	-	++	++++	++++	++++

Key: - insoluble, + partially soluble, ++ soluble, +++ very soluble, ++++ extremely soluble

4.2 Characterization of the synthesized compounds

4.2.1 Elemental Analysis

The structural formulas of the synthesized ligands and corresponding metal complexes were also established with the aid of their elemental analysis (Table 2) and this was done by comparing the mass percentage compositions of elements (carbon, hydrogen and nitrogen) theoretically calculated to that experimentally found. The elemental analysis is in agreement with the formulas proposed for the ligand and corresponding metal complexes because the theoretical calculated element composition percentage values of carbon, hydrogen and nitrogen in respective compounds are close if not the same with the values of such elements experimentally found by this procedure. In addition elemental analysis also provided aid in determining the molecular weight of synthesized compounds and later revealed which reaction molar ratio (2:1 or 1:1 ligand to metal) favored the synthesis of the compounds. Figure 8 and 9 show the proposed structures of the synthesized ligands that corresponds to the elemental analysis data and by considering the starting materials' structures.

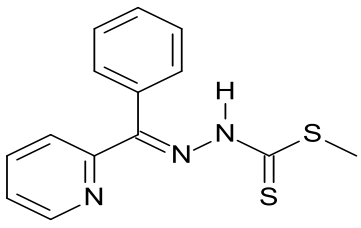

Figure 7: The structure of HL^1 ligand

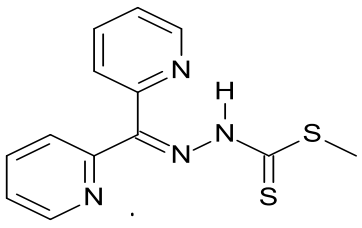

Figure 8: The structure of HL^2 ligand

For HL^1 complexes of cadmium(II), iron(II), zinc(II) and nickel(II), their elemental analysis outcomes are consistent with the proposition having a 1:2 metal to ligand molar ratio, whereas the elemental analysis result of cobalt(II) and copper(II) complexes of HL^1 indicates that these two complexes has a metal to ligand reaction molar ratio of 1:1. All the metal (cadmium(II), zinc(II), and copper (II)) complexes of HL^2 displayed elemental analysis results in agreement with a metal to ligand molar ratio of 1:1 except for nickel (II) complex of the same ligand which agreed to a 1:2 molar ratio.

4.2.2 ^{1}HNMR

Further evidence in support of the formation of the ligands and their corresponding metal complexes is obtained from ^{1}HNMR data of figure 9-12 (also in appendix A) and displayed in table 4 and 5. The concept used in assigning absorption signal peaks to respective proton on the compounds' structure is based on which proton is more close to electron withdrawing groups (such as nitrogen) which is expected to appear more downfield and vice versa. Each individual ligand (HL^1 and HL^2) with its corresponding metal complexes in DMSO solution were found to provide the same signal peaks at nearly if not the same chemical shift with their corresponding metal complexes. However there is an exception for the absence of N^2-H signal peak at about δ=14.4 ppm and δ=15.11 ppm (in HL^1 and HL^2 respectively) in corresponding metal complexes. The later hence imply that the deprotonation of the ligand has indeed occurred. In both spectrums of ligands and their corresponding metal complexes the signal peak appearing further up-field at about δ=2.50 ppm is a result of the DMSO solution that was used to analyze the samples. Since that there are no

huge differences between the signal peaks of ligands and their corresponding metal complexes, not all the spectra of the metal complexes (figure 11 and 12) are shown. The rest of the later spectra are shown under appendices section.

4.2.2.1 ^{1}HNMR spectra of HL^{1} ligand

The ^{1}HNMR spectra of HL^{1} ligand shown in figure 9 were analyzed and their signal peak positions are shown in table 4.

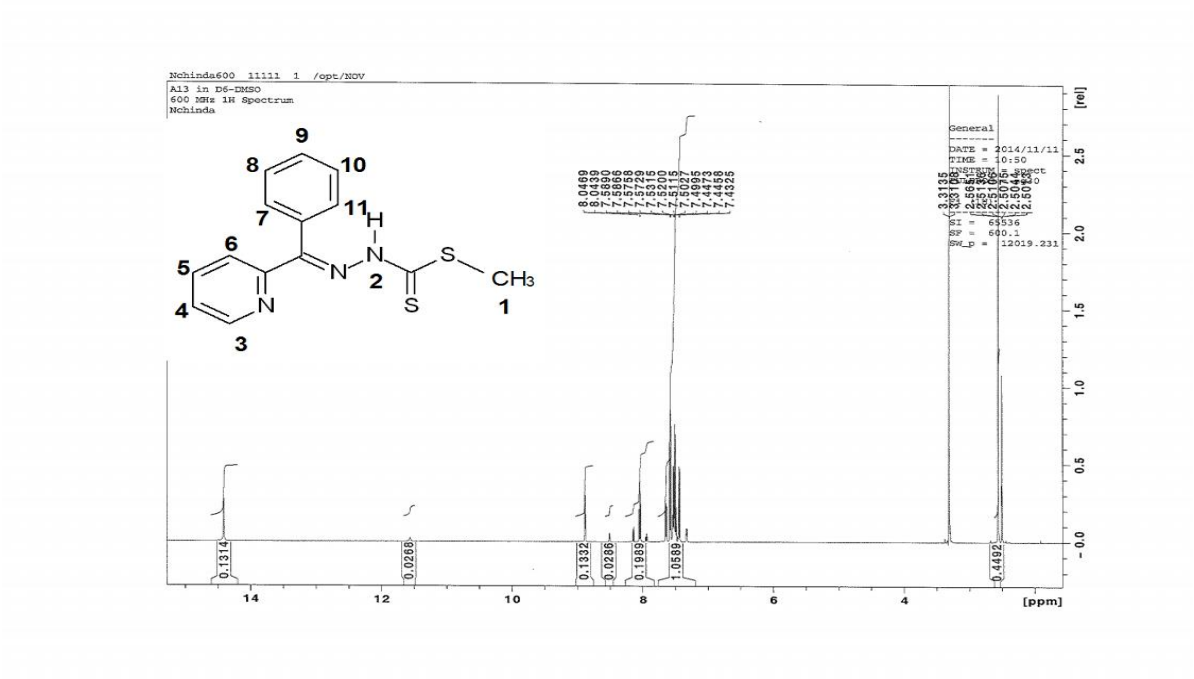

Figure 9: The ^{1}HNMR spectra peaks of HL^{1} structure with assigned protons

The signal exhibited downfield at δ=14.4 ppm is a characteristic of N^{2}-H (Ali *et al*., 2007). The signal peaks appearing more up-field at δ=3.31 ppm is due to methyl protons of C^{1}-H$_3$ (Ali *et al*., 2011). The signal peaks integrated at about chemical shifts (δ) of 7.52 ppm, 7.50 ppm, 7.49 ppm, 7.51 ppm and 7.53 ppm are due to aromatic phenyl group (How *et al*., 2008). The protons of C^{4}-H and C^{5}-H may be

assigned to the signal peak at about δ=8.18 ppm and δ=7.99 ppm respectively. The signal peaks at a chemical shifts of about δ=8.50 ppm may be assigned to the pyridine protons of C^6-H while that at δ=8.85 ppm may be assigned to proton of C^3-H.

Table 4: The ^{1}HNMR spectrum HL^1 ligand

^{1}HNMR of HL^1			
Position of peaks by chemical shift (δ) (ppm)	Hydrogen as assigned in figures	Assignment	Numbers of protons
14.4	2	N^2-H	1
3.31	1	C^1-H_3	3
7.52, 7.50, 7.49, 7.51, 7.53	7, 8, 9, 10, 11	Phenyl (C^7-H, C^8-H, C^9-H, C^{10}-H, C^{11}-H)	5
8.18, 7.99	4, 5	Pyridine (C^4-H and C^5-H)	2
8.50	6	Pyridine (C^6-H)	3
8.85	3	Pyridine (C^3-H)	1

4.2.2.2 ^{1}HNMR spectra of HL^2 ligand

The ^{1}HNMR spectrum of HL^2 (figure 10) displayed absorption in the chemical shift region of 0–15 ppm. The signal peaks situated more up-field at δ=3.31 ppm is due to methyl protons of C^1-H_3 (Ali *et al*., 2011). The signal exhibited at δ=14.4 ppm is a characteristic of N^2-H (Ali *et al*., 2007). In correlation to the similar absorption peak in HL^1 (figure 9), the signal peaks appearing as an integration at about δ = 8.85 ppm may be assigned to symmetrical pyridyl protons of C^3-H and C^{10}-H which are in the same chemical environment, while that at about δ=8.65 ppm may be as a result of the pyridine proton of C^6-H and C^7-H.

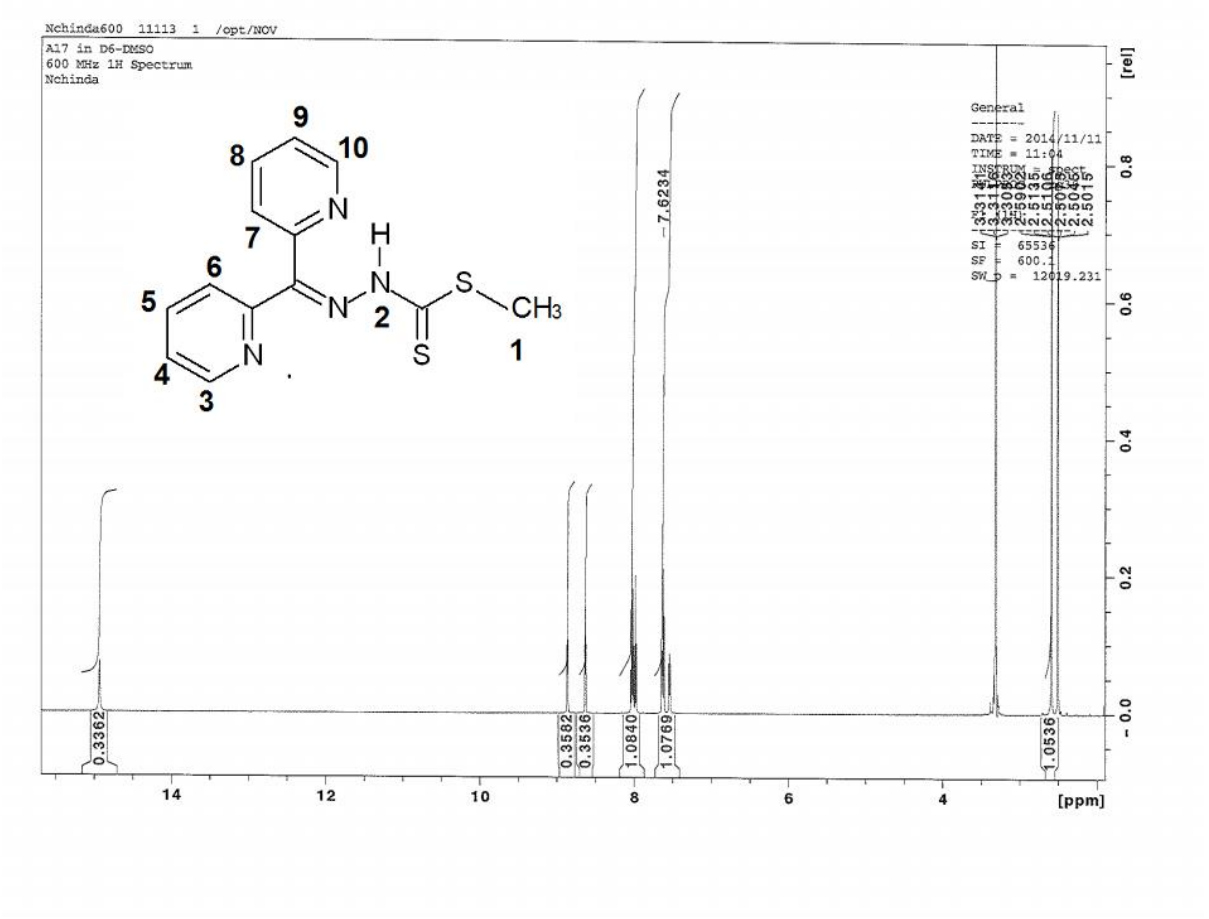

Figure 10: The ^{1}HNMR spectra peaks of HL^{2} structure with assigned protons

Table 5: The ^{1}HNMR spectrum of HL^{2} ligand

^{1}HNMR of HL^{2}			
Position of peaks by chemical shift (δ) (ppm)	Hydrogen as assigned	Assignment	Numbers of protons
15.11	2	N^{2}-H	1
3.31	1	C^{1}-H_3	3
8.85	3,10	Pyridyl (C^{3}-H, C^{10}-H)	2
8.65	6,7	Pyridyl (C^{6}-H, C^{7}-H)	2
8.00	4,9	Pyridyl (C^{4}-H, C^{9}-H)	2
7.65	5,8	Pyridyl (C^{5}-H, C^{8}-H)	2

Other two pairs of protons on this structure that are in the same chemical environment are symmetrical C^4-H and C^9-H producing signal peaks at about δ = 8.0 ppm and protons of C^5-H and C^8-H producing signal peaks integrating at about δ = 7.65 ppm (Ali *et al*., 2011) (table 5). (Ali *et al*. 2011).

4.2.2.3 ^{1}HNMR spectra of metal complexes of HL^1 and HL^2 ligands

The metal complexes were prepared using a two (metal to ligand) molar reaction ratio of 2:1 and 1:1. The ^{1}HNMR spectra of copper (II) and nickel (II) complexes when compared to that of their respective free ligands (HL^2 and HL^1), shows a huge downward shifts of the positions. The signal bands of downfield shifted positions are broader in complexes whereas in the free ligands they are sharply intense and this can be due to the paramagnetic shift in such complexes. In copper (II) complexes of HL^1 even though the position of phenyl (C^7-H, C^8-H, C^9-H) shifted up-field from 7.5 ppm in ligand to 6.74 ppm in a complex, the position of pyridine (C^4-H, C^5-H, C^6-H) shifted downfield from 8.00 in ligand to 8.705 ppm in complex while that of pyridine (C^4-H) greatly shifted from 8.043 in ligand to 9.4339 ppm in complex. The signal peak positions of nickel complex of HL^1 both shifted downward with phenyl (C^7-H, C^8-H, C^9-H) shifting from 7.5 ppm in ligand to 8.82 in complex, whereas pyridine (C^4-H, C^5-H, C^6-H) shifted from 8.0 ppm in ligand to 9.1 ppm in complex and pyridine (C^4-H) position hugely shifted from 8.5 ppm in ligand to 12.5 ppm in complex. The copper (II) and nickel (II) complexes of HL^2 similarly also shows a downfield shifts of the positions of pyridyl (C^3-H, C^{10}-H), pyridyl (C^4-H, C^5-H, C^6-H) and pyridyl (C^7-H, C^8-H, C^9-H) protons with different chemical environment for each signal peak position of ligand in its comparison to that of its complex

respectively.

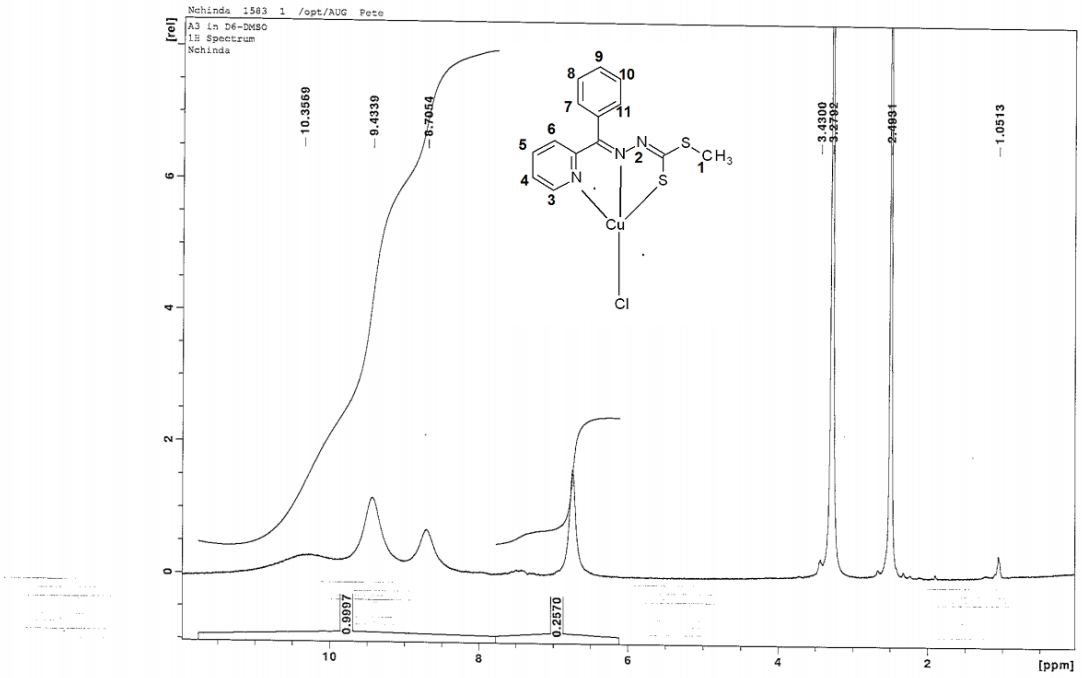

Figure 11: Structure of CuL^{1}_{2} with its assigned hydrogen numbers.

Despite the d^8 and d^7 copper(II) and nickel(II) complexes respectively, the electronic spectra of the d^{10} zinc (II) and cadmium (II) complexes are similar to those of the respective free ligands although bathochromic shifts of the bands seen in the free ligands are apparent (Ali *et al*., 2007). However the downshift of signal peak position of free ligand in comparison to that of their corresponding metal complexes is ascribed to the coordination of the ligands to the corresponding metal center through pyridine nitrogen, azomethine nitrogen and thiolate sulphur atoms (Bera *et al*., 2008). The later effects is that it reduces the electron density at these atoms to different paramagnetic extend (Bera *et al*., 2008). Also complexion of free ligand to metals is

supported by the spectrum in DMSO of all the metal complexes of both ligands which does not display bands corresponding to N-H and S-H, hence proving that the ligands have been deprotonated (Takjoo & Centore 2012). Consequently confirming the presence of thiolate form of the ligand in the complexes (Takjoo & Centore 2012). As a result the producing metal complexes of the empirical formula ML_2 (for a metal to ligand reaction molar ratio of 1:2) and MLX (for a metal to ligand reaction molar ratio of 1:1), where M= Ni^{2+}, Cu^{2+}, Co^{2+}, Cd^{2+}, Zn^{2+}, and Fe^{2+}, L=deprotonated ligand and X=Cl.

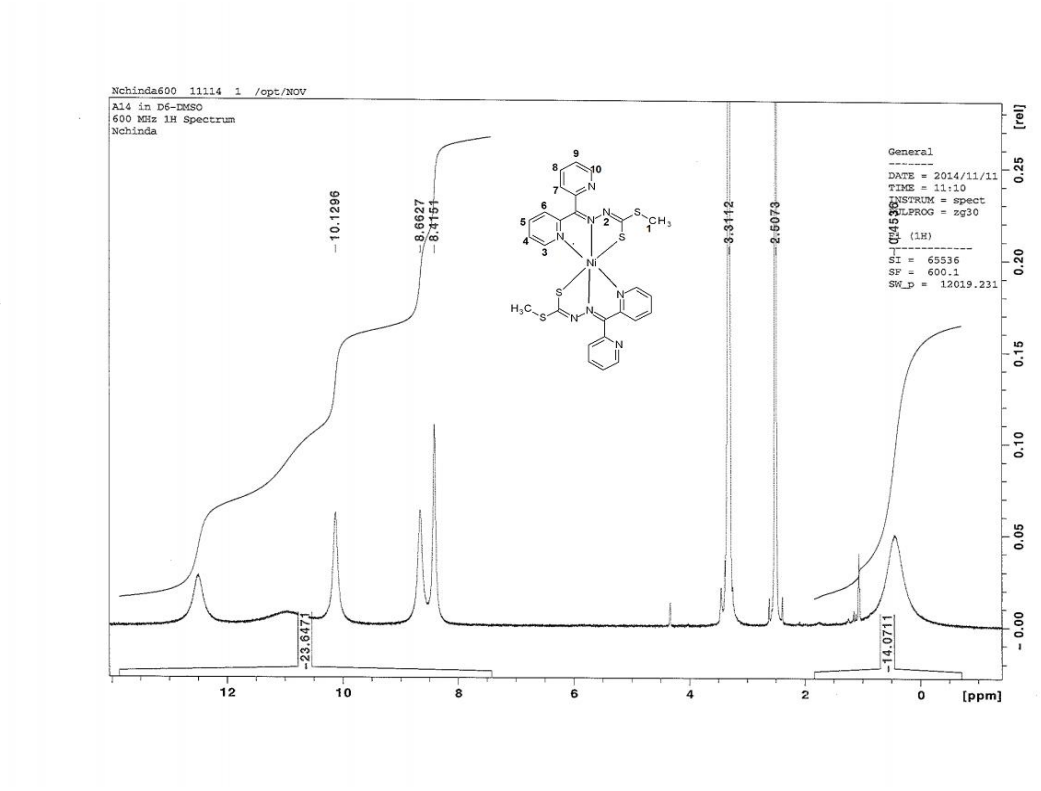

Figure 12: structure of NiL^2_2 with its assigned hydrogen numbers

4.3 Infrared Spectroscopy

The IR spectra of both ligands and metal complexes where obtained from solid samples and the data extracted from the spectrum are shown in table 6 and 7. The major IR bands of the compounds were identified on the basis of similar compounds (Li *et al*., 2011). The significant IR absorption bands of the ligands and their corresponding metal complexes and their assignments are displayed in table 7.

Table 6: Infrared absorption frequencies (cm^{-1}) of synthesized compounds

Ligands	**Metal complexes of HL^1**			
HL^1	$FeL^1{}_2$	CoL^1Cl	$NiL^1{}_2$	$CdL^1{}_2$
3680w,sh 3540w 3400w,b 3210w,b 3025w,b 2400m 1600w 1500s 1425s 1400s 1350m 1300m 1225m 1100s 1050s 950m 800s 750s 750m 700m 690s 600m	3900w 3800w,b 3400w 3050w 2350m 1400s 1325s 1140w 1050m 950m 825w 750m 700m 650w 625m	3750w 3500w 3300w 3050w 1600w 1500w 1400s 1350s 1200w 1125s 1000s 950m 800m 750m 700m 650s 625m 600m	3950w,3100 w 2350w 1600w 1425w 1400s 1300s 1100s 1000m 800m 750m 700m 650w 600m	3675w 3400w 3150w 1750w 1600w 1400s 1300m 1148s 1000w 975s 800s 750m 700m 650w
	Metal complexes of HL^2			
HL^2	CuL^2Cl	$NiL^2{}_2$		CdL^2Cl
3700w, 3615w, 3000w,b,2900b, 2400w, 2350m, 1600m,1560m, 1500m, 1430s, 1425s, 1400s, 1350m, 1250m,sh, 1150s,sh, 1100s, 1025s, 1000s, 950m, 900w,sh, 800s, 750m, 689s	3850w 3450w, 3300w 2355w, 1600w 1475w 1400s 1350m 1150w 1100s 1000s 950m 900w 800m 750m 650m	3850w 3625w 3050w 1600m 1455m 1425m 1400s 1300s 1100s 1000s 750m 600m		3850m 3600m 3100w,b 2350m 1600m 1400s 1300s 1250m 1100s 950s 800m 750m 650m

Peak descriptions: s=strong, m=medium, w=weak, sh=sharp, and b=broad.

Table 7: Significant analyzed IR absorption spectra synthesized compounds.

	Assignments						
Compounds	*v*(N-H)	*v*(C-H)	*v*(C=N) + *v*(C=C)	*v*(N-N)	*v*(C-N) + *v*(C=S)	*v*(C-S)	Py
HL^1	3540w 3400w,b	3210w,b	1425s 1400s	1225m	1100s 1050s		690s
$FeL^1{}_2$	3400w	3050w	1400s	1325s	1050m	1140w	650w
CoL^1Cl	3500w 3300w	3050w	1600w 1500w 1400s	1350s 1200w	1000s	1125s	650s
$NiL^1{}_2$		3100w	1600w 1425w 1400s		1000m	1100s	650w
$CdL^1{}_2$	3400w	3150w	1600w 1400s	1300m	1000w	1148s	650w
HL^2	3615w,	3000b, 2900b,	1500m,1425s, 1400s,1600m	1250sh,m,	1025s, 1000s		689s
CuL^2Cl	3450w 3300w		1600w 1475w 1400s	1350m	1000s	1150w 1100s	650m
$NiL^2{}_2$	3625w	3050w	1600m 1455m 1425m 1400s	1300s	1000s	1100s	
CdL^2Cl	3600m	3100w,b	1600m 1400s	1300s 1250m	950s	1100s	650m

The starting materials for the formation of HL^1 and HL^2 are hydrazide derivative and 2-benzoylpyridine and 2-di-pyridyl ketones respectively. The formation of the ligands is confirmed by the absence of the absorptional band at 1760-1665 cm^{-1} and 3200-3180 assignable to *v*(C=O) and *v*(NH_2) of ketone and hydrazine functional groups (Chan *et al*., 2007). The IR spectra of ligands in the region of 1400-1000 cm^1 are similar to their corresponding metal complexes due to similar organic functional group present in both ligand and their corresponding metal complexes (Daniel, 2009).

The IR spectra of the metal complexes, when compared with the free ligands spectrum show significant modifications that can be correlated with the metal

complex formation. The IR spectra of the free ligands (HL^1 and HL^2) do not exhibit a *v*(S-H) band at around 2700 cm^{-1} but show broad and weak absorption bands at 3400 cm^{-1} for HL^1 and 3615 cm^{-1} for HL^2 attributable to *v*(N-H), hence this indicates that in the solid state, the ligands remains in the thione form (Chan *et al*., 2007).

The infrared spectral bands most useful for determining the mode of coordination of the ligands are v(C=N), *v*(N-N) and v(C=S) vibrations (Li *et al*., 2011). A comparison of the IR spectra of the ligands with their corresponding metal complexes indicates that the *v*(N-H) bands off the free ligands observed at 3400 cm^{-1} for HL^1 and 3615 cm^{-1} for HL^2 are not present in the spectra of the complexes supporting deprotonation of the ligands during coordination. The breathing motion of pyridine ring is shifted to a higher frequency upon complexation and is consistent with pyridine ring nitrogen coordination (Li *et al*., 2011)

In addition, Li *et al.* (2011) who studied the same ligands for investigation against selected bacteria and fungi argues that the shift of the *v*(C=N) bands of the free ligands to lower wavenumbers and the shift of *v*(N-N) bands to higher wavenumbers in the IR spectra of the complexes support coordination of the ligands to the metal atom via the azomethine nitrogen atom. However the latter is not surprising since the v(C=N) band is expected to couple with other bands and its shifting will depend on how much it is in combination with these bands, and as such it is not a reliable indicator of the coordination mode (Ali *et al*., 2011). HL^1 and HL^2 shows *v*(C=S) modes at 1050s cm^{-1} and 1025 cm^{-1} respectively (table 7). In the spectra of the complexes, the v(C=S) modes observed in ligands disappeared in corresponding complexes and the frequencies shown in table 7 under the column of *v*(C-N) +

v(C=S) can only be attributed to *v*(C-N) bands of metal complexes (Li *et al*., 2011). Consequently the *v*(C-S) modes are observed at about 1100 cm^{-1} and 1150 cm^{-1} in metal complexes and not in their corresponding ligands confirming that complexion has occurred. Based on the above spectral evidences, it is confirmed that the free ligands are tridentate, coordinating via pyridyl nitrogen, azomeethine nitrogen and the thiolato sulphur atoms (Li *et al*., 2011).

4.4 The suggested structural formulae of the synthesized ligands and their corresponding metal complexes.

The following structural compounds (figure 14-24) were formulated and experimentally confirmed by their analytical (EA), spectral data (^{1}HNMR) and FT-IR spectra.

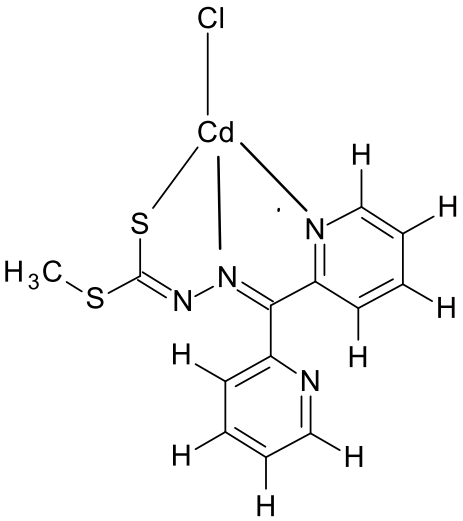

Figure 13: The structure of CdL^2Cl

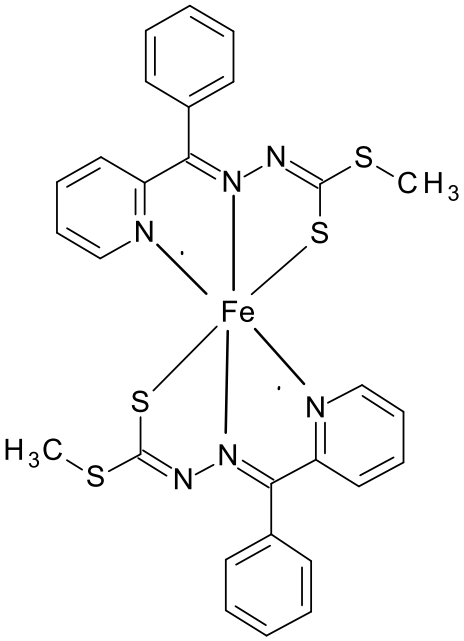

Figure 14: The structure of FeL^1_2

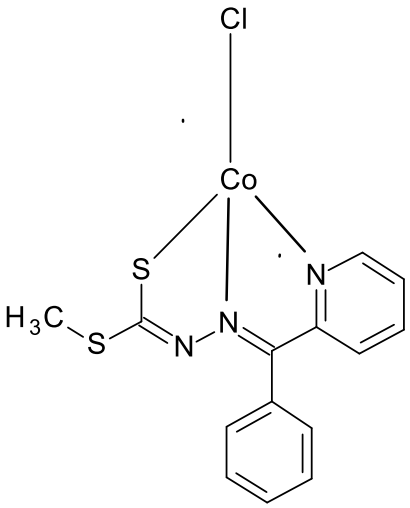

Figure 15: The structure of CoL^1Cl

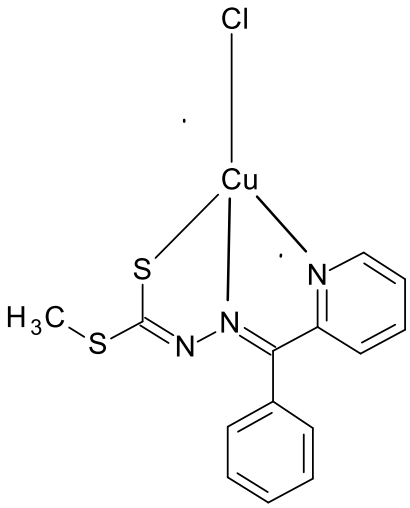

Figure 16: The structure of CuL^1Cl

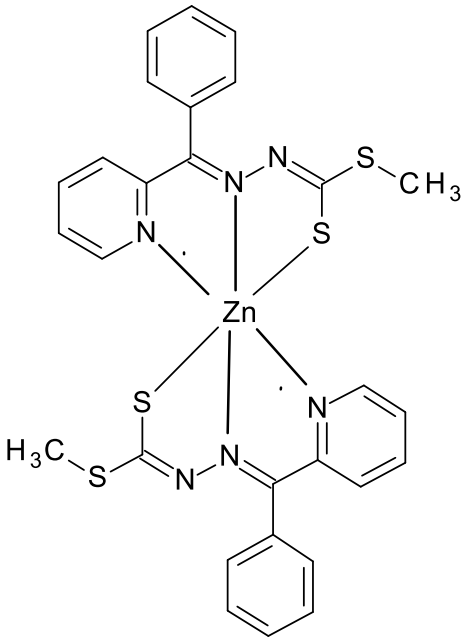

Figure 17: The structure of ZnL^1_2

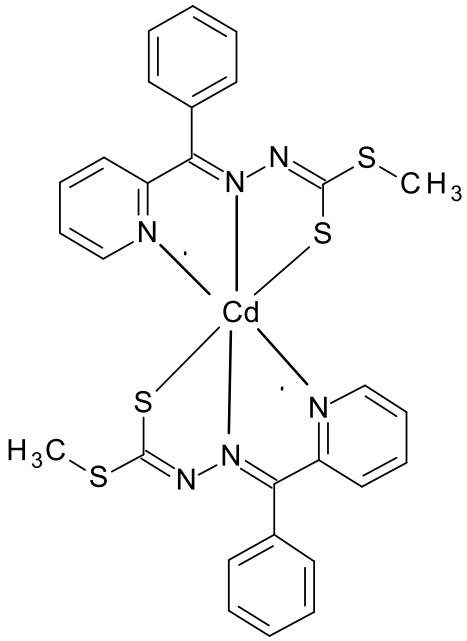

Figure 18: The structure of CdL^1_2

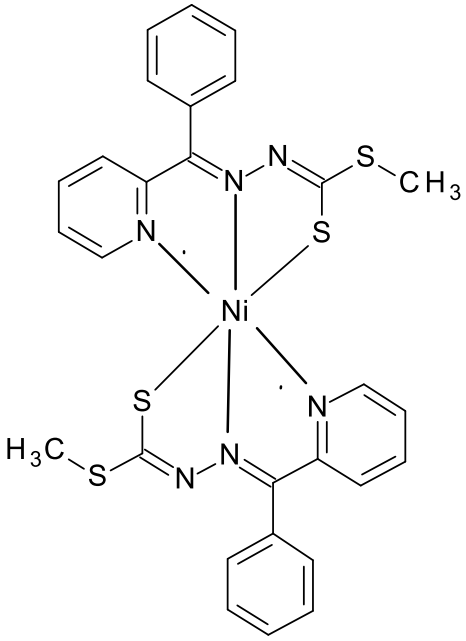

Figure 19: The structure of NiL^1_2

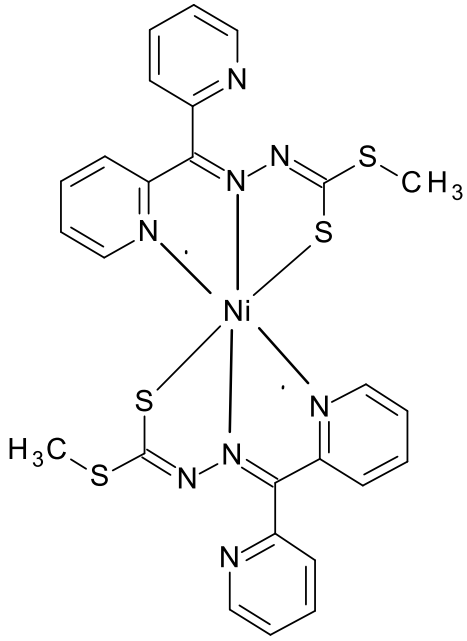

Figure 20: The structure of NiL^2_2

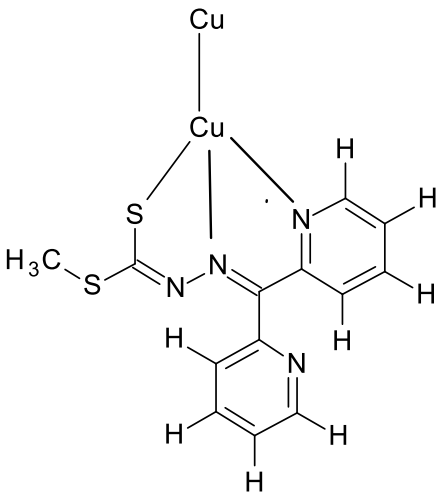

Figure 21: The structure of CuL^2Cl

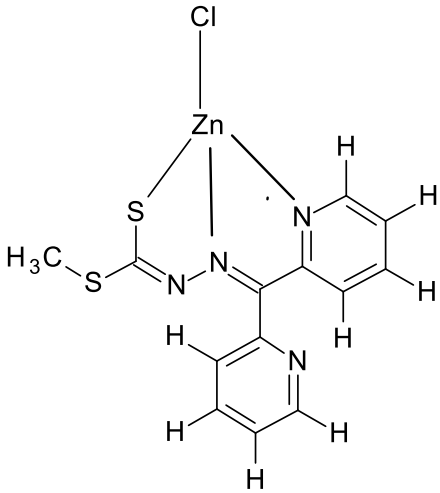

Figure 22: The structure of ZnL^2Cl

4.5 The antimalarial assay

With exception of Zn (II) complex of HL^1 all the synthesized compounds were assayed for antimalarial activity. The *in vitro* technique was employed by screening the compounds for antiplasmodial activity against *P. falciparum* chloroquine sensitive (CQS) NF54 strain. Chloroquine and Artesunate compounds of quinone family were used as a control in screening the synthesized compounds. The antiplasmodial activities of the compounds were measured in nanogram per mililiter (ng/ml) unit by the half inhibitory concentration (IC_{50}).

Biological evaluation of the two synthesized ligands and their corresponding metal complexes against malaria parasite are illustrated in table 8. The lower the NF54:IC_{50} (ng/ml) ratio the strong the biological activity of the compound is toward *P. falciparum*. The data depicted that HL^1 and its corresponding copper complex showed strong activities towards *P. falciparum* while HL^2 ligand and its corresponding metal complexes showed very weak activities toward the same parasite. In comparison to chloroquine and artesunate (control compounds) with IC_{50} values of 3.06±0.64 ng/ml and <2.00±ND ng/ml respectively, it can confidently be assumed that strong antiplasmodial activity of HL^1 than HL^2 can be structurally attributed to the fact that HL^2 (with an IC_{50} value of 19.3±2.0 ng/ml) contains an extra pyridine group in comparison to HL^1 (with an IC_{50} value of 2.23±0.24 ng/ml). The reason for later could be that the additional pyridine group may decrease the antiplasmodial activity of HL^2. The result also shows that HL^1 ligand possesses greater half inhibitory concentration (2.23±0.24 ng/ml) against *P. falciparum* NF54 strain compared to upon its complexion with most metal ions and this implies that

the complexion decreases the antiplasmodial activity of HL^1 ligand toward the same strain.

Table 8: *In vitro* antiplasmodial activity against *P. falciparum* (CQS) NF54 strain

Compounds	**NF54:IC_{50} (ng/ml)**
HL^1	2.23±0.24
$FeL^1{}_2$	222±23.6
CoL^1Cl	66.7±0.94
CuL^1Cl	4.43±0.31
$NiL^1{}_2$	69.0±8.2
$CdL^1{}_2$	6.03±1.49
HL^2	19.3±2.0
CuL^2Cl	20.8±4.3
ZnL^2Cl	21.7±2.5
$NiL^2{}_2$	208±22.7
CdL^2Cl	19.7±5.3
CQ	3.06±0.64
Artesunate	<2.0±ND

Metal complexes of HL^1 ligand like CuL^1Cl and $CdL^1{}_2$ contain better half inhibitory concentration with values of 4.43±0.31 and 6.03±1.49 ng/ml compared to the controls. According to Qiu *et al*. (2014) not many copper complexes have been studied for their biological activities such as anticancer property and recent studies have demonstrated that certain multinuclear Cu(II) complexes can efficiently promote DNA cleavage by hydrolyzing the phosphate linkage. In contrary CoL^1Cl and $NiL^1{}_2$ exhibited decreased IC_{50} values of 66.7±0.94 and 69.0±8.2 ng/ml compared to controls. More ever, nickel which has been proven to be the bioelement

of mankind plays an important role in hormone, metabolism and stability of biological macromolecules and in particular, planar nickel(II) complexes are coordinately unsaturated and can act as Lewis acids; the anticancer and antimicrobial activities of many nickel complexes may be related with that feature (Mashra *et al*., 2013; Qiu *et al*., 2014). However FeL^1_2 proved to have the lowest half inhibitory concentration with IC_{50} value of 222±23.6 ng/ml compared to the controls and this could be that the compound was very impure and further recrystallization is recommended for this compound.

Even though all the metal complexes of HL^2 ligand showed low or decreased half inhibitory concentration towards the *P. falciparum* NF54 strain compared to the controls, its however also observed that the ligand (with IC_{50} value of 19.3±20 ng/ml) have a high antiplasmodial activity than its corresponding metal complexes like CdL^2Cl, CuL^2Cl and ZnL^2Cl with IC_{50} value of 19.7±5.3, 20.8±4.3 and 21.7±2.5 ng/ml respectively. The later could still be due to that complexion decreases the antiplasmodial activity of HL^2 ligand toward the same strain. NiL^2_2 with IC_{50} value of 208±22.7 ng/ml in comparison to controls did in fact revealed the lowest antiplasmodial activity towards the strain and this could be due to that the compound was not pure and hence further double recrystallization is recommended for the compound.

CHAPTER 5: CONCLUSION

This study overseen the synthesis of two ligand systems of Schiff's base ligands namely; 2-benzoylpyrine-s-methyldithiocarbazate and di-2-pyridylketone-s-methyldithiocarbazate (HL^1 and HL^2 respectively) and their reaction coordination with some transition metal ions such as copper (II), zinc (II), cadmium (II), nickel (II), iron (II) and cobalt (II). The ligands and their metal complexes were synthesized using acid catalyzed condensation reaction method and characterized using techniques of EA, FT-IR and ^{1}HNMR.

On the basis of the available physicochemical properties, FT-IR and ^{1}HNMR, it can be reasonably concluded that HL^1 and HL^2 ligands coordinated in their deprotonated form through one of the pyridine nitrogen atom, the azomethine nitrogen atom and the thiolate sulfur. Subsequently confirming that HL^1 and HL^2 behaved as tridentate *N, N, S* chelate with all coordinated respective metal ions centers (zinc, cadmium, nickel, copper, iron, silver and manganese), as envisaged by spectroscopic (FT-IR and ^{1}HNMR) and analytical data (EA). However synthesized metal complexes that were favored by a ligand-metal 2:1 reaction molar ratio coordinated in an octahedral environment while these favored by a 1:1 reaction molar ratio coordinated in a trigonal bipyramid environment completed by a chloride atom.

The synthesized ligands and their corresponding metal complexes were tested for antiplasmodial activity against the chloroquine sensitive NF54 strain line of *P. falciparum*. Overall HL^1 ligand was found to be more biological active against NF54 strain of *P. falciparum* than its corresponding metal complexes and counterpart HL^2 (and its corresponding metal complexes). The latter could be that the extra pyridine

group in HL^2 can be accounted for the decrease in antiplasmodial activity of this ligand. Metal complexes of HL^1 also exhibited increased biological activities than these of HL^2 ligand for the same reason that HL^1 is more antiplasmodial active than HL^2. Despite that there are metal complexes (cadmium and copper) with moderate half inhibitory concentration against the same strain, importantly it can also be concluded that the complexion with metal ions decreases the antiplasmodial activity of the ligands. Therefore the two synthesized free ligands are at the advantage of being lead compounds against antiplasmodial activity than their corresponding metal ions reported under this study.

Recommendations

Despite the Elemental Analysis, FT-IR and HNMR used in structural identification of the synthesized compounds, the coordination circumstances between ligand and metal complexes is also better determined by EI-MS (which is useful for the unequivocal characterization of large molecules). Hence for future reference it is recommended that EI-MS is done on these or similar compounds for better structural identification. The synthesized ligands and their corresponding metal complexes under this study proved to have antiplasmodial activity against NF54 strain line of *P. falciparum*. However their IC_{50} values vary, as these of ligands decreased upon complexion. It is therefore recommended that upon developing a lead compound of antiplasmodial activity, ligands under this study are of more powerful effect alone than they are with corresponding metal complexes and so as some metal complexes of HL^1 (cadmium and copper) compared to HL^2 ligand. This study can be continued in future to test and study the toxicity level of the synthesized compounds with valuable antiplasmodial activity.

CHAPTER 6: REFFERENCES

Alegana, V. A., Atkinson, P. M., Wright, J. A., Kamwi, R., Uusiku, P., Katokele, S., Noor, A. M. (2013). Estimation of malaria incidence in northern Namibia in 2009 using Bayesian conditional-autoregressive spatial–temporal models. *Spatial and Spatio-temporal Epidemiology*, 30(6), 26-29.

Ali, M. A., Mirza, A. H., Bakar, J. H. A., & Bernhardt, P. V. (2011). Preparation and structural characterization of nickel (II), cobalt (II), zinc (II) and tin (IV) complexes of the isatin Schiff bases of S-methyl and S-benzyldithiocarbazates. *Polyhedron*, 30(4), 556-564.

Ali, M. A., Mirza, A. H., Butcher, R. J., Bernhardt, P. V., & Karim, M. R. (2011). Self-assembling dicopper (II) complexes of di-2-pyridyl ketone Schiff base ligands derived from S-alkyldithiocarbazates. *Polyhedron*, 30(9), 1478-1486.

Ali, M. A., Mirza, A. H., Hamid, M. H., Aminath, N., & Bernhardt, P. V. (2012). Synthesis, characterization and X-ray crystal structures of thiolate sulfur-bridged dimeric copper(II) complexes of the 2-aminoacetophenone Schiff base of S-methyldithiocarbazate Malai Haniti S.A. *Polyhedron*, 30(10), 79-86.

Arulmurugan, S., Kavitha, H. P., & Venkatraman, R. P. (2010). Biological activities of Schiff base and its complexes: *a review. Rasayan J Chem*, 3(3), 385-410.

Bahl, D., Athar, F., Botelho, M., Soares, P., Santos, M., Sá, D., Azam, A. (2010). Bioorganic & Medicinal Chemistry Structure – activity relationships of mononuclear metal – thiosemicarbazone complexes endowed with potent antiplasmodial and antiamoebic activities. *Bioorganic & Medicinal Chemistry*, 18(18), 6857–6864. http://doi.org/10.1016/j.bmc.2010.07.039

Bera, P., Kim, C. H., & Seok, S. I. (2008). Synthesis, spectroscopic characterization and thermal behavior of cadmium (II) complexes of S-methyldithiocarbazate (SMDTC) and S-benzyldithiocarbazate (SBDTC): X-ray crystal structure of [Cd (SMDTC) 3]· 2NO 3. *Polyhedron*, 27(17), 3433-3438.

Bloland, P. B. (2001). Drug resistance in malaria. *World Health Organisation*, 1-27.

Chan, M. H. E., Crouse, K. A., Tahir, M. I. M., Rosli, R., Umar-Tsafe, N., & Cowley, A. R. (2008). Synthesis and characterization of cobalt (II), nickel (II), copper (II), zinc (II) and cadmium (II) complexes of benzyl N-[1-(thiophen-2-yl) ethylidene] hydrazine carbodithioate and benzyl N-[1-(thiophen-3-yl) ethylidene] hydrazine carbodithioate and the X-ray crystal structure of bis {benzyl N-[1-(thiophen-2-yl) ethylidene] hydrazine carbodithioate} nickel (II). *Polyhedron*, 27(4), 1141-1149.

Chellan, P., Nasser, S., Vivas, L., Chibale, K., & Smith, G. S. (2010). Cyclopalladated complexes containing tridentate thiosemicarbazone ligands of biological significance: Synthesis, structure and antimalarial activity. *Journal of Organometallic Chemistry*, 695(19), 2225-2232.

Dabrowiak, J. C. (2012). Metals in Medicine. *Inorganica Chimica Acta*, 15(4), 1-7.

Daniel, L. S. (2009). *The synthesis and characterization of copper (II) complexes containing thiosemicarbazone and semicarbazone ligands derived from ferrocene and pyridyl fragments.* Retrieved from http://repository.unam.na/handle/11070/453

de Lima, R. L., Teixeira, L. R., Carneiro, T. M., & Beraldo, H. (1999). Nickel(II), Copper(I) and Copper(II) Complexes of Bidentate Heterocyclic Thiosemicarbazones. *Journal of Brazillian Chemistry Society*, 24(8), 184-189.

de Oliveira, R. B., de Souza-Fagundes, M. E., Soares, P. P. R, Andrade, A. A., Krettli, A. U., & Zani, L. C. (2007). Synthesis and antimalarial activity of semicarbazone and thiosemicarbazone derivatives. *European Journal of Medicinal Chemistry*, 43, 1983-1988.

Eissa, H. H., (2013). Synthesis, Characterization and Antibacterial Activity of Macrocyclic Schiff Bases Based on 1, 3-Docarbonyl Phenyl Dihydrazide, 1, 4-Docarbonyl Phenyl Dihydrazide. *Organic Chem Curr Res*, *2*(122), 2161-0401.

Garoufis, A., Hadjikakou, S. K., & Hadjiliadis, N. (2009). Palladium coordination compounds as anti-viral, anti-fungal, anti-microbial and anti-tumor agents. *Coordination Chemistry Reviews*, 35(23), 1384-1385.

How, F. N. F., Crouse, K. A., Tahir, M. I. M., Tarafder, M. T. H., & Cowley, A. R. (2008). Synthesis, characterization and biological studies of S-benzyl-β-N-(benzoyl) dithiocarbazate and its metal complexes. *Polyhedron*, 27(15), 3325-3329.

Huang, R., Wallqvist, A., & Covell, D. G. (2005). Anticancer metal compounds in NCI's tumor screening database: putative mode of action. *Biochemical Pharmacology*, 15(4), 1009-1014.

Hussain, Z., Yousif, E., Ahmed, A., & Altaie, A. (2014). Synthesis and characterization of Schiff's bases of sulfamethoxazole. *Organic and medicinal chemistry letters*, 4, (1), 23-27.

Kiremire, E. (2010). Method of synthesizing a complex active against the malaria parasite plasmodium falciparum. *US Patent App. 13/642,615*. Retrieved from http://www.google.com/patents/US20130137871

Kizilcikli, I., Kurt, Y. D., Akkurt, B., Genel, A. Y., Birteksöz, S., Ötük, G., & Ülküseven, B. (2007). Antimicrobial activity of a series of thiosemicarbazones and their ZnII and PdII complexes. *Folia microbiologica*, 52(1), 15-25.

Kumar, S., & Kumar, N. (2013). Synthesis and biological activity of acetylacetone thiosemicarbazone and their metallic complexes. *International Current Pharmaceutical Journal*, 88(9), 17-23.

Laufer, M. K., Thesing, P. C., Eddington, N. D., Masonga, R., Dzinjalamala, F. K., Takala, S. L., ... & Plowe, C. V. (2006). Return of chloroquine antimalarial efficacy in Malawi. *New England Journal of Medicine*, 355(19), 1959-1966.

Li, M. X., Chen, C. L., Ling, C. S., Zhou, J., Ji, B. S., Wua, Y. J., & Niu, J. Y. (2009). Cytotoxicity and structure–activity relationships of four a-N-heterocyclic thiosemicarbazone derivatives crystal structure of 2-acetylpyrazine thiosemicarbazone. *Bioorganic & Medicinal Chemistry Letters*, 104(3), 2704-2709.

Li, M. X., Zhang, L. Z., Chen, C. L., Niu, J. Y., & Ji, B. S. (2012). Synthesis, crystal structures, and biological evaluation of Cu (II) and Zn (II) complexes of 2-benzoylpyridine Schiff bases derived from S-methyl-and S-phenyldithiocarbazates. *Journal of inorganic biochemistry*, 106(1), 117-125.

Lobana, T. S., Kumari, P., Hundal, G., & Butcher, R. J. (2010). Metal derivatives of N 1-substituted thiosemicarbazones with divalent metal ions (Ni, Cu): Synthesis and structures. *Polyhedron*, 29(3), 1130-1136.

Mishra, A., Kumar, N., Sardar, M., & Sahal, D. (2013). Colloids and Surfaces B : Biointerfaces Evaluation of antiplasmodial activity of green synthesized silver nanoparticles. *Colloids and Surfaces B: Biointerfaces*, 111, 713–718. http://doi.org/10.1016/j.colsurfb.2013.06.036

Ott, I. (2009). On the medicinal chemistry of gold complexes as anticancer drugs. *Coordination Chemistry Reviews*, 25(4), 1670-1677.

Pavan, F. R., Maia, P. I. D. S., Leite, S. R., Deflon, V. M., Batista, A. A., Sato, D. N., & Leite, C. Q. (2010). Thiosemicarbazones, semicarbazones, dithiocarbazates and hydrazide/hydrazones: Anti–Mycobacterium tuberculosis activity and cytotoxicity. *European journal of medicinal chemistry*, 45(5), 1898-1905.

Pelosi, G. (2010). Thiosemicarbazone Metal Complexes: From Structure to Activity. *The Open Crystallography Journal*, 16(8), 143-148.

Pingaew, R., Supaluk, P., & Ruchirawat, S. (2010). Synthesis, Cytotoxic and Antimalarial Activities of Benzoyl Thiosemicarbazone Analogs of Isoquinoline and Related Compounds. *Molecules*, 43(5), 989-994.

Qiu, X. Y., Zhang, C., Li, S. Z., Cao, G. X., Qu, P., Zhang, F. Q., Zhai, B. (2014). Synthesis, crystal structures and cytotoxic activity of mononuclear nickel(II) and dinuclear zinc(II) complexes with ligand derived from S-benzyldithiocarbazate. *Inorganic Chemistry Communications*, 46, 202–206. http://doi.org/10.1016/j.inoche.2014.05.015

Saifi, M. A., Beg, T., Harrath, A. H., Altayalan, F. S. H., & Al Quraishy, S. (2013). Antimalarial drugs: Mode of action and status of resistance. *African Journal of Pharmacy and Pharmacology*, 7(5), 148-156.

Sayin, U., Turkkan, E., Dereli, O., Yuksel, H., & Birey, M. (2010). EPR study of gamma-irradiated single crystal 4-phenylsemicarbazide. *Radiation Physics and Chemistry*, 79(8), 863-869.

Scovill, J. P., Klayman, D. L., Lambros, C., Childs, G. E., & Notsch, J. D. (1983). 2-Acetylpyridine Thiosemicarbazone as Potential Antimalarial Agents1p2. *journal of medicinal chemistry*, 87(4), 243-248.

Steel, M. (2001). Oxford wordpower dictionary. New York, USA: *Oxford University press*.

Takjoo, R., & Centore, R. (2013). Synthesis, X-ray structure, spectroscopic properties and DFT studies of some dithiocarbazate complexes of nickel (II).*Journal of Molecular Structure*, 1031, 180-185.

Yousef, T. A., El-Gammal, O. A., Ahmed, S. F., & El-Reash, G. A. (2015). Synthesis, biological and comparative DFT studies on Ni (II) complexes of NO and NOS donor ligands. *Spectrochimica Acta Part A: Molecular and Biomolecular Spectroscopy*, 135, 690-703.

APPENDICES

APPENDIX A: ^{1}HNMR SPECTRA

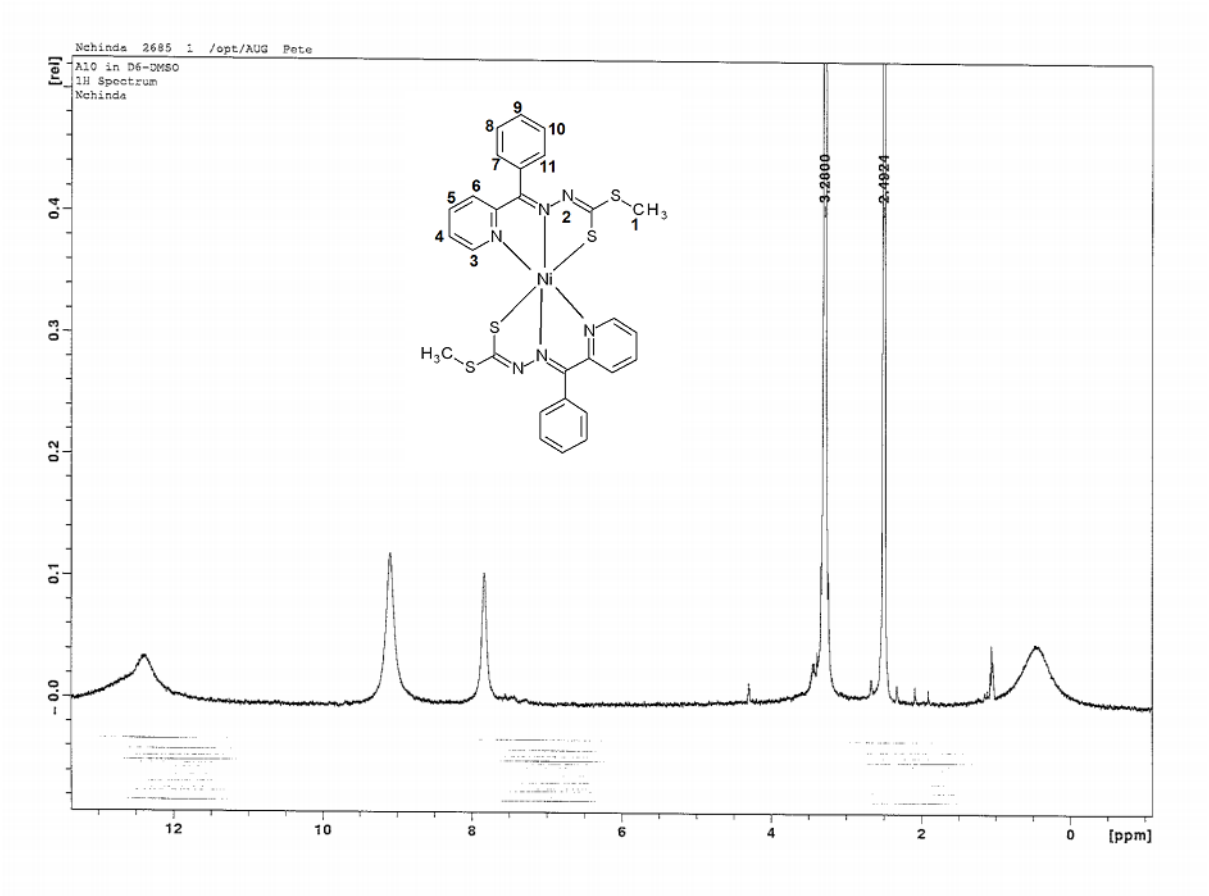

Appendix A$_1$: ^{1}HNMR spectrum of NiL^{1}_{2}

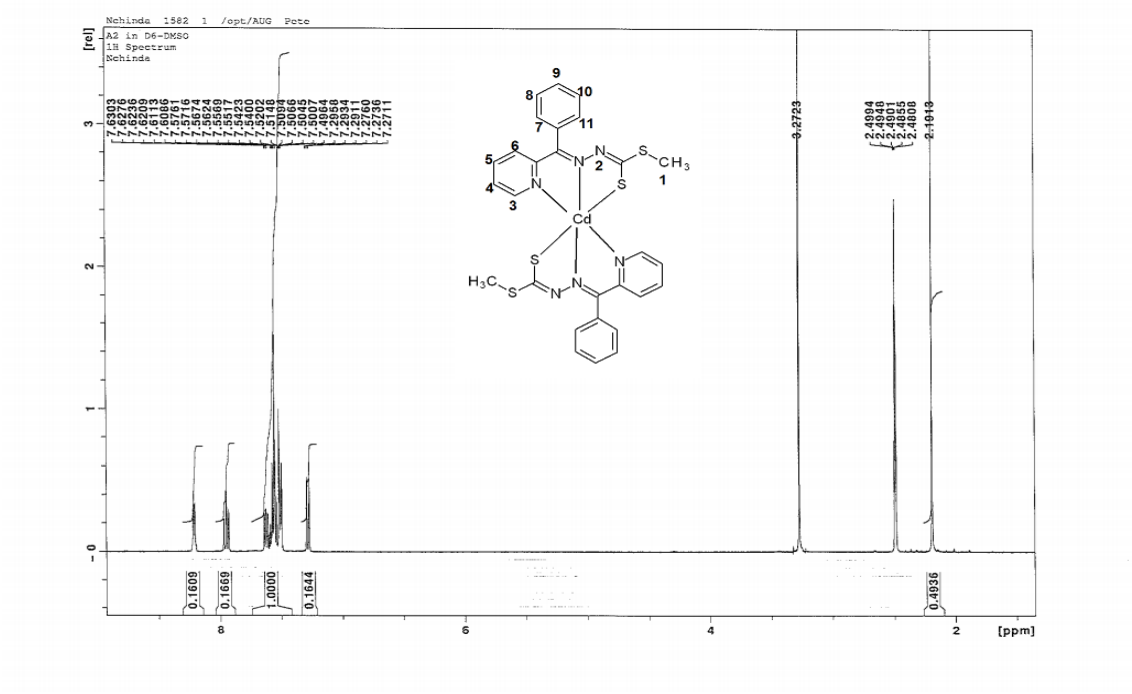

Appendix A₂: ^{1}HNMR spectrum of CdL^{1}_{2}

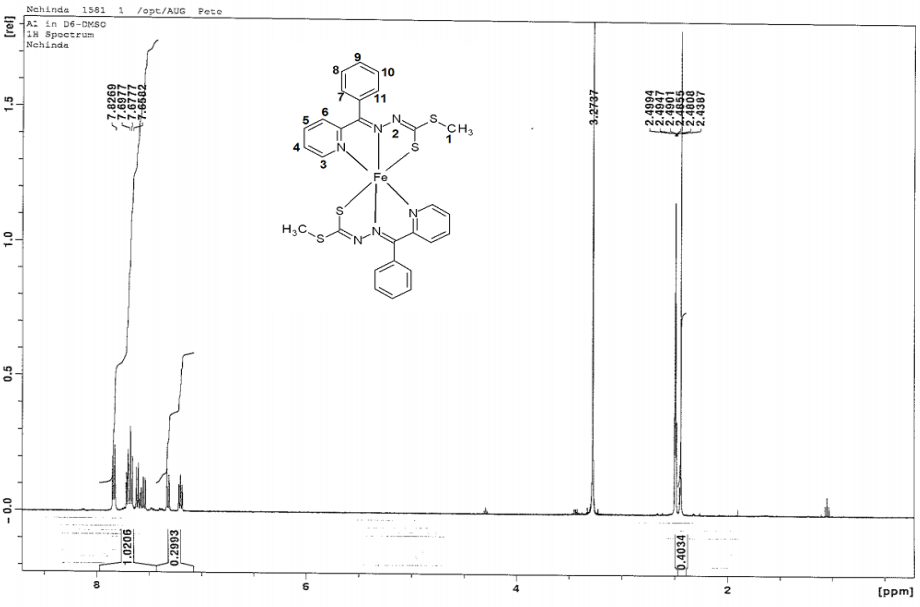

Appendix A₃: ^{1}HNMR spectrum of FeL^{1}_{2}

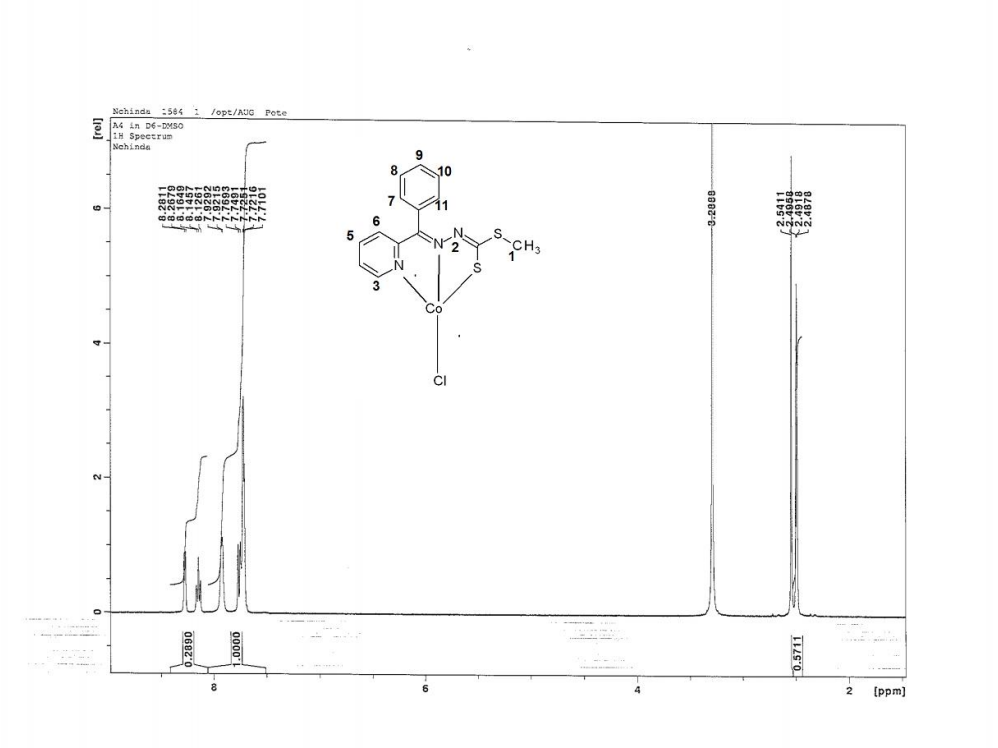

Appendix A₄: ^{1}HNMR spectrum of $CoL^{1}Cl$

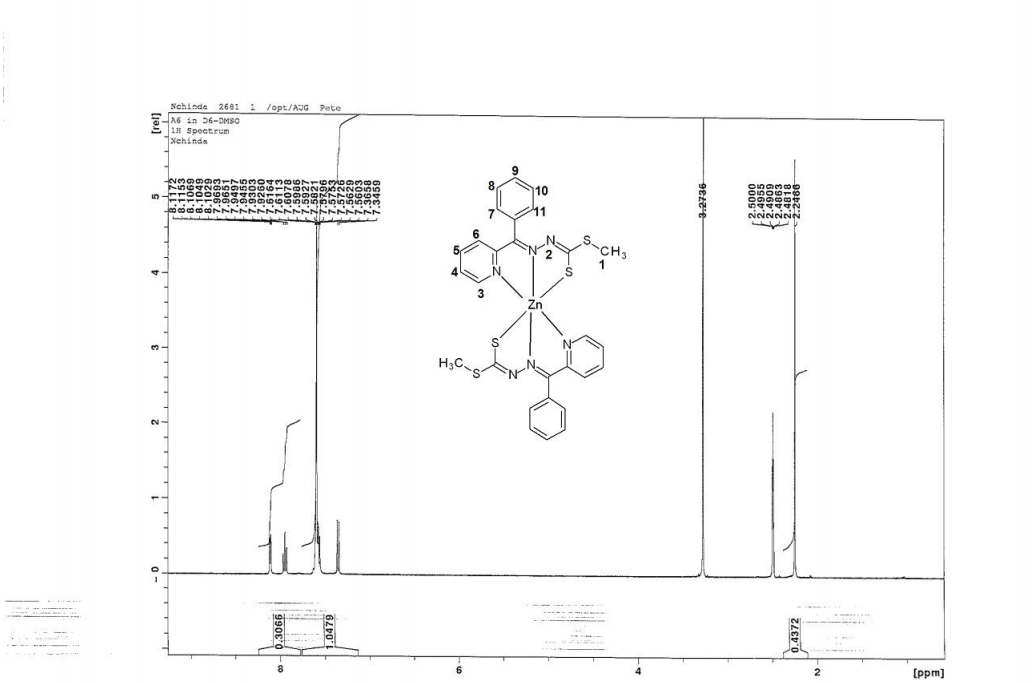

Appendix A₅: ^{1}HNMR spectrum of ZnL^{1}_{2}

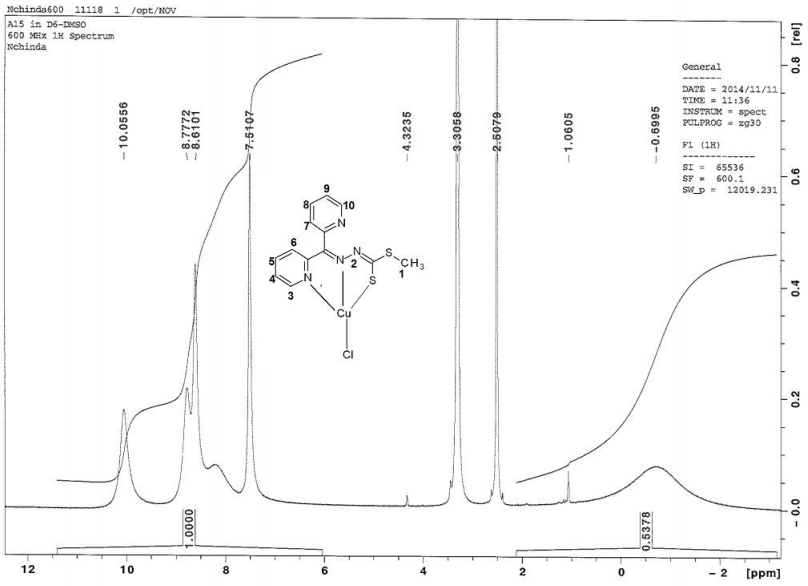

Appendix A6: ^{1}HNMR spectrum of $CuL^{2}Cl$

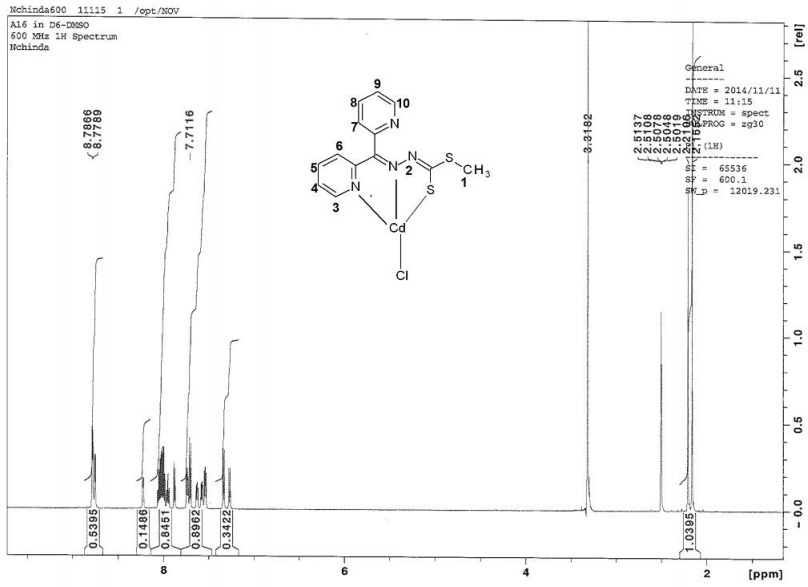

Appendix A7: ^{1}HNMR spectrum of $CdL^{2}Cl$

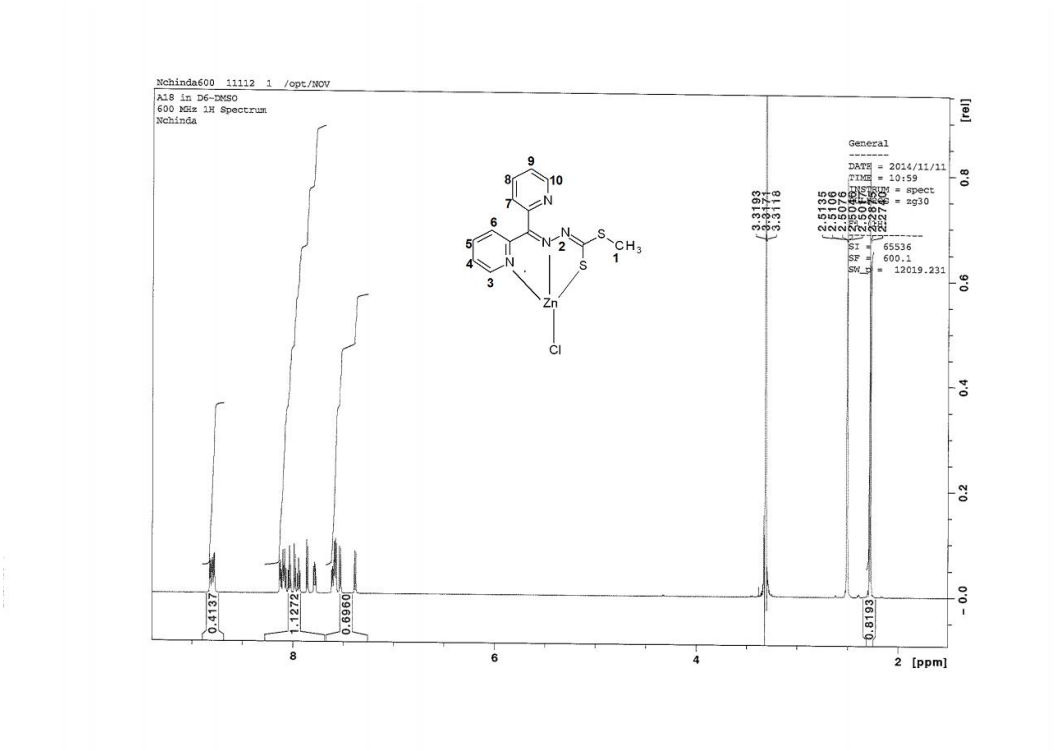

Appendix A8: ^{1}HNMR spectrum of $ZnL^{2}Cl$

APPENDIX B: FT-IR SPECTRA

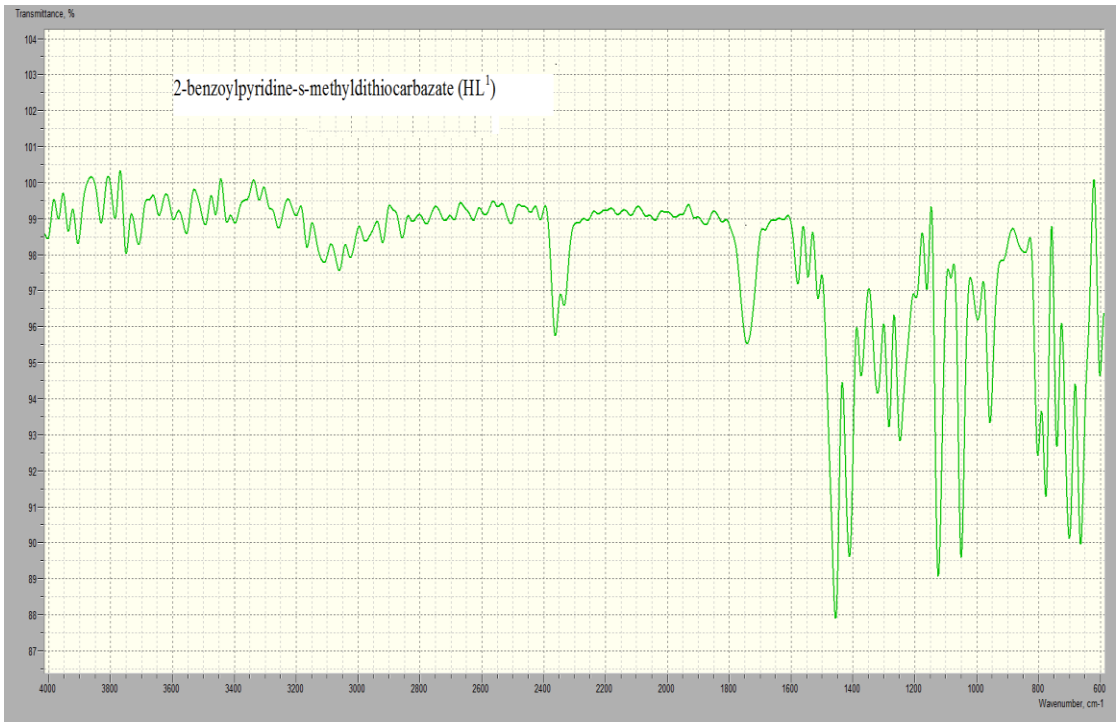

Appendix B$_1$: FT-IR spectra of HL[1]

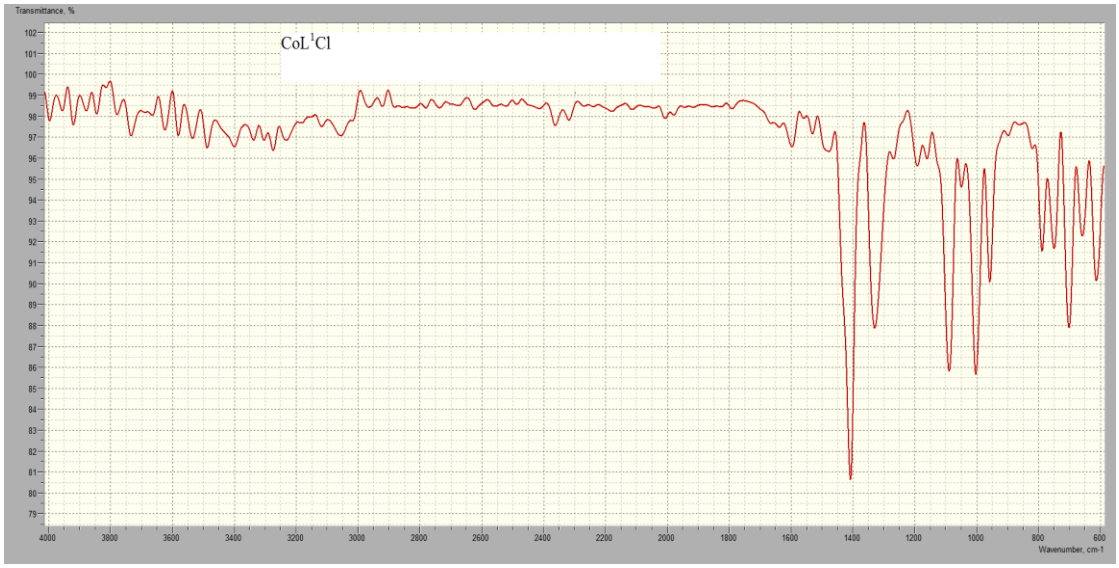

Appendix B2: FT-IR spectra of CoL^1Cl

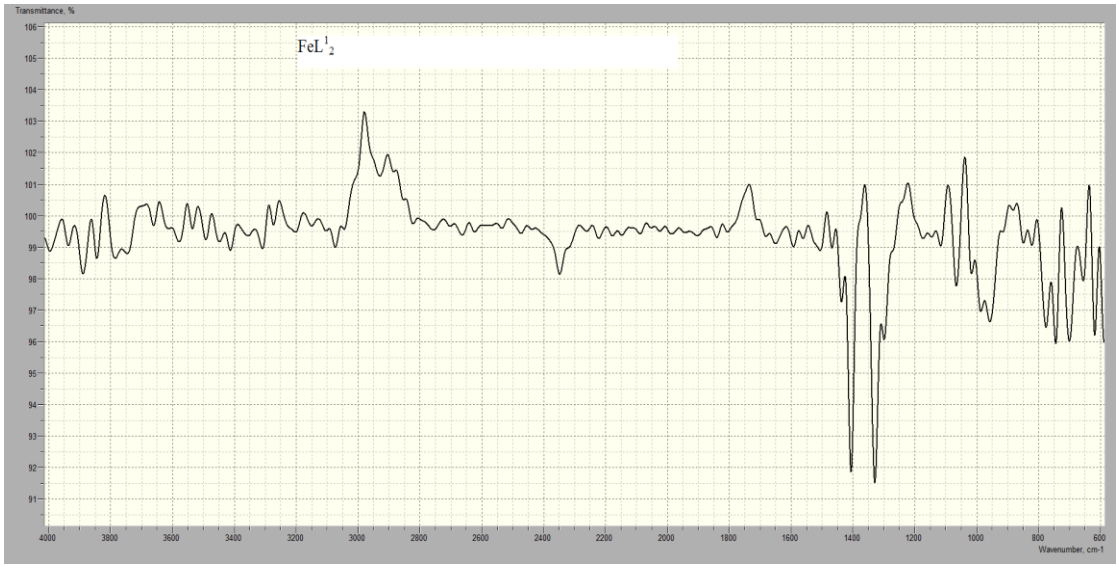

Appendix B3: FT-IR spectra of $FeL^1{}_2$

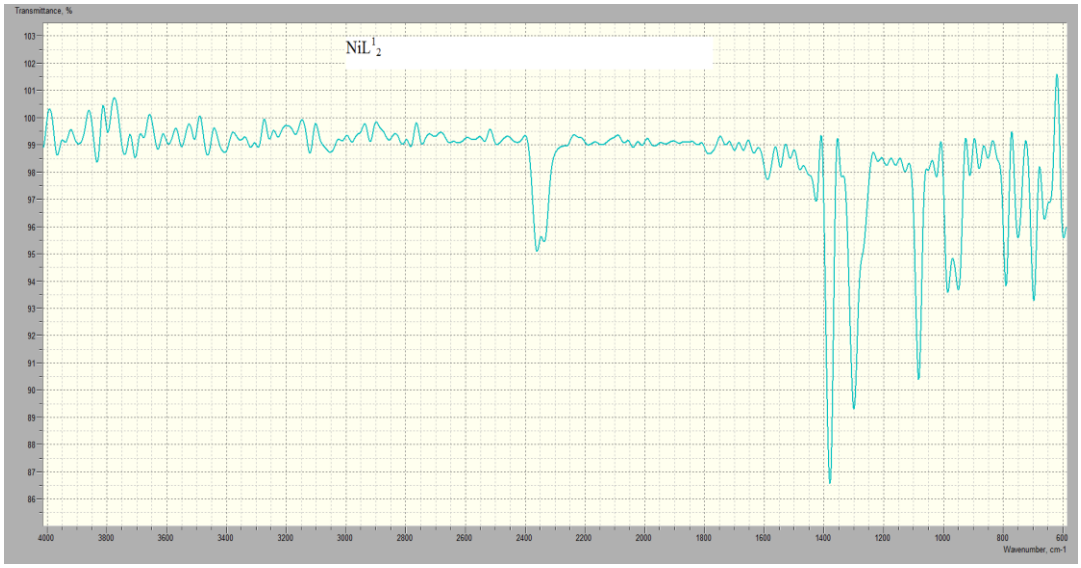

Appendix B₄: FT-IR spectra of NiL^1_2

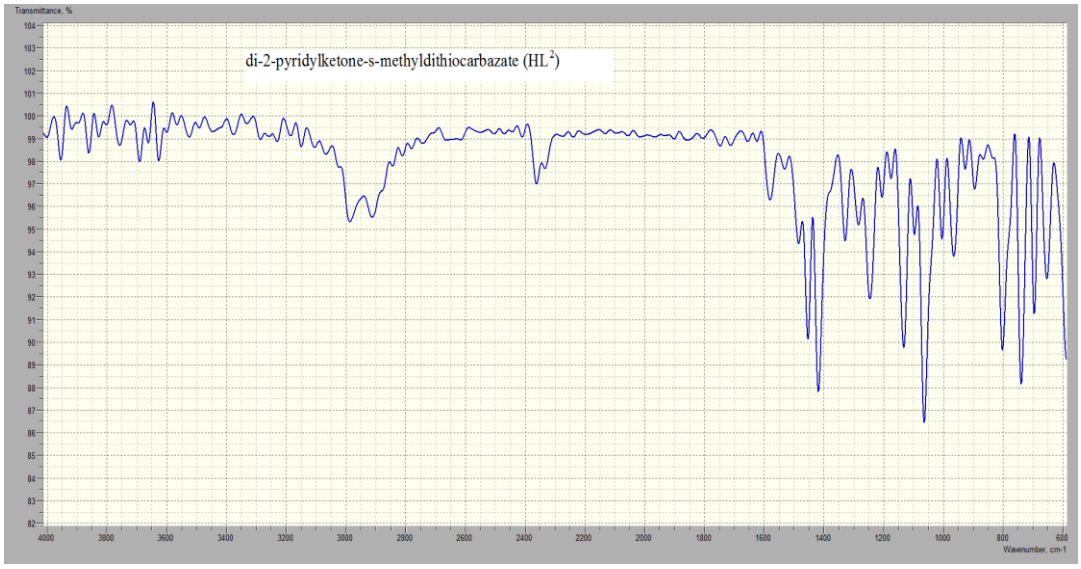

Appendix B₅: FT-IR spectra of HL^2

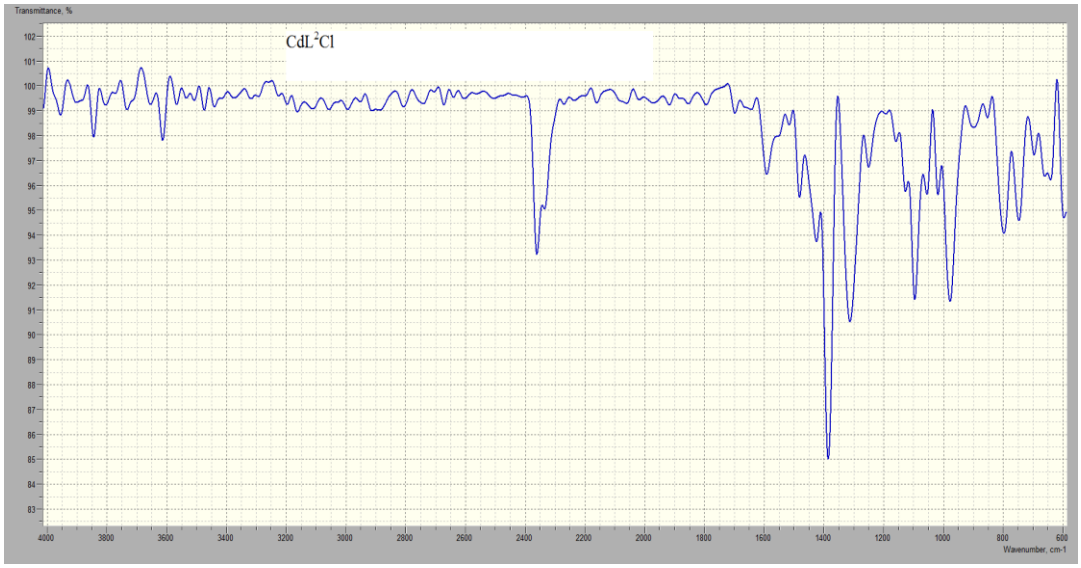

Appendix B6: FT-IR spectra of CdL^2Cl

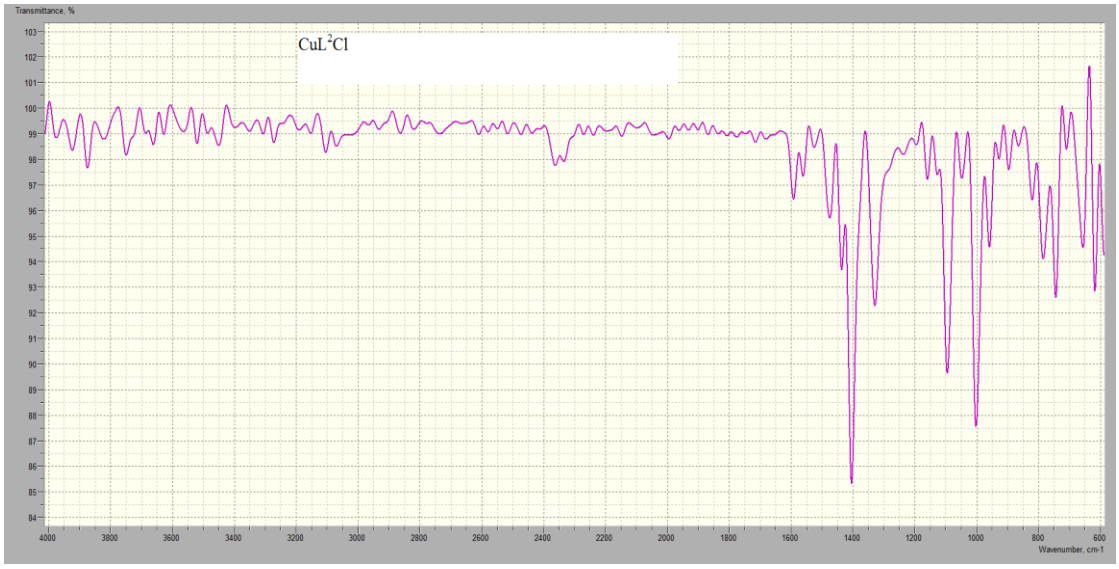

Appendix B7: FT-IR spectra of CuL^2Cl

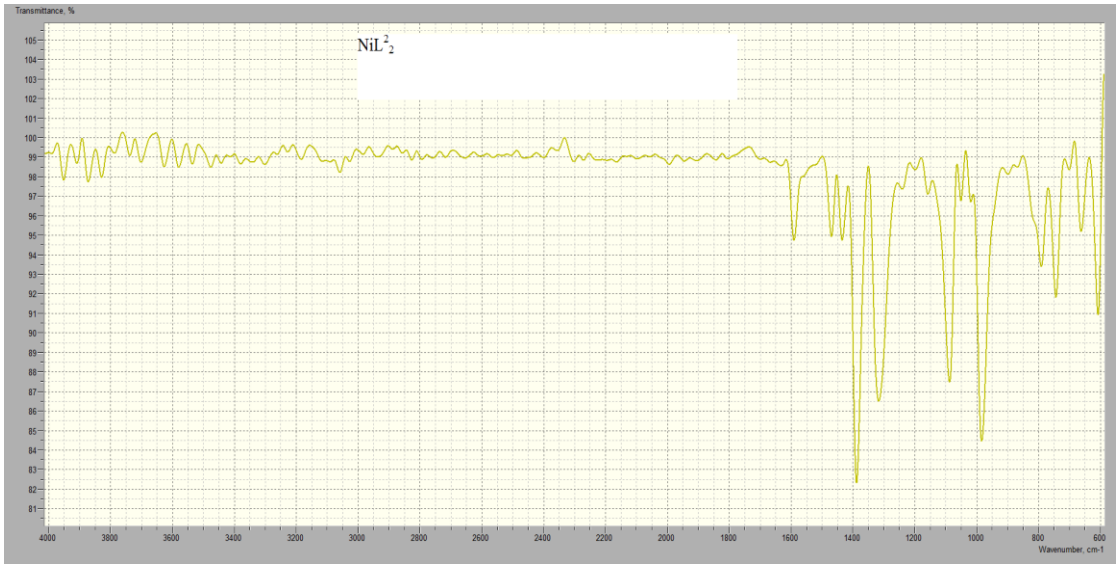

Appendix B$_8$: FT-IR spectra of NiL$^2_2$

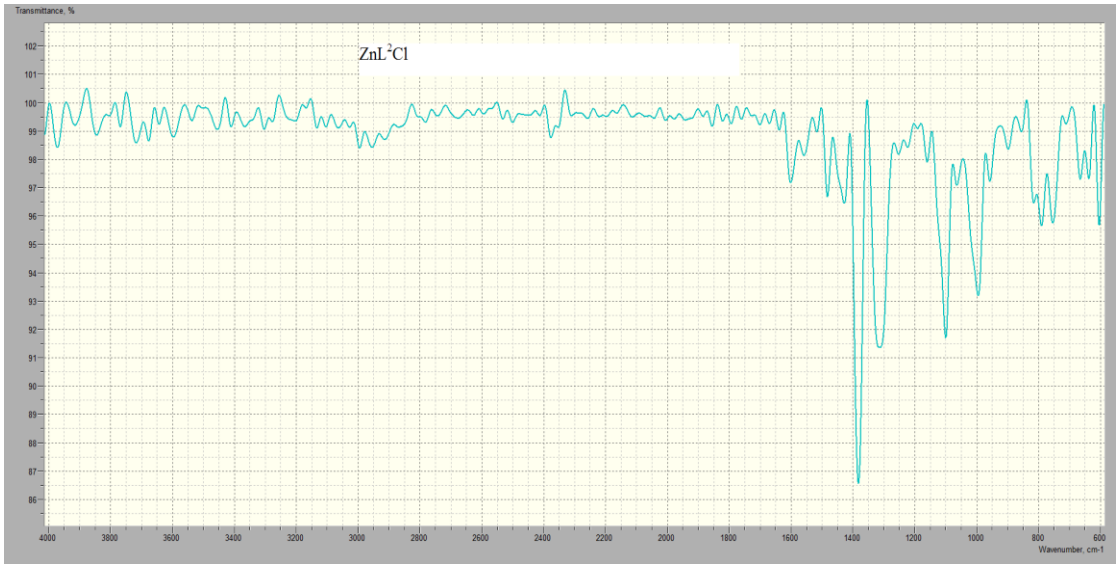

Appendix B$_9$: FT-IR spectra of ZnL^{2}Cl